Functional nanostructured materials for stormwater runoff treatment

Ko, Dongah

Publication date:
2017

Document Version
Publisher's PDF, also known as Version of record

Functional nanostructured materials for stormwater runoff treatment

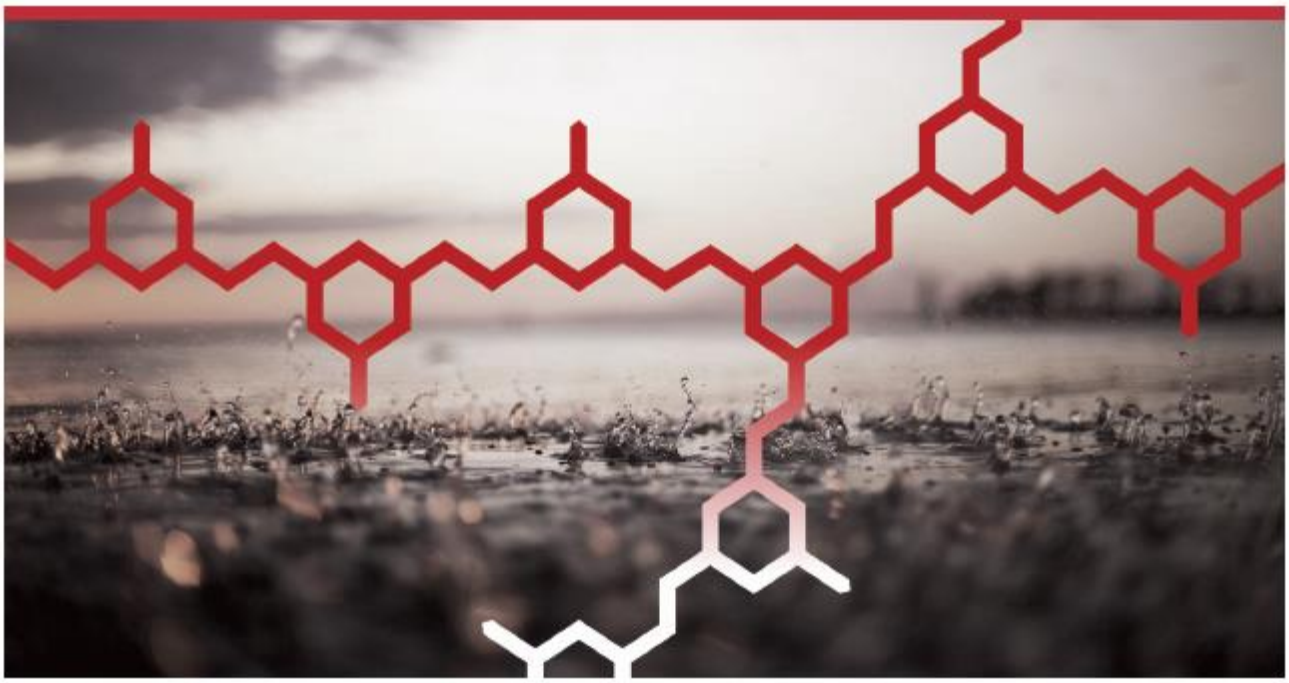

Dongah Ko

PhD Thesis
December 2017

DTU Environment
Department of Environmental Engineering

Functional nanostructured materials for stormwater runoff treatment

Dongah Ko

PhD Thesis
December 2017

DTU Environment
Department of Environmental Engineering
Technical University of Denmark

Functional nanostructured materials for stormwater runoff treatment
Dongah Ko

PhD Thesis, December 2017

The synopsis part of this thesis is available as a PDF file for download from the DTU research database ORBIT: http://www.orbit.dtu.dk.

Address:	DTU Environment Department of Environmental Engineering Technical University of Denmark Bygningstorvet, Building 115 2800 Kgs. Lyngby Denmark
Phone reception:	+45 4525 1600
Fax:	+45 4593 2850
Homepage:	http://www.env.dtu.dk
E-mail:	reception@env.dtu.dk
Cover:	Donghyeon Hong

Preface

This dissertation, entitled "Functional nanostructured materials for stormwater runoff treatment," comprises research carried out in the Department of Environmental Engineering at the Technical University of Denmark, the Department of Micro- and Nanotechnology at the Technical University of Denmark and the Graduate School of EEWS at the Korea Advanced Institute of Science and Technology (KAIST) between December 2014 and December 2017. The research was conducted under the supervision of Professor Henrik R. Andersen at DTU Environment, and co-supervision was supplied by Associate Professor Cafer T. Yavuz at KAIST EEWS, Associate Professor Mogens H. Jakobsen at DTU Nanotech and Assistant Professor Yuhoon Hwang at Seoul National University of Science and Technology.

The thesis is organised in two parts: the first puts into context the findings of the PhD in an introductive review, while the second part consists of the papers listed below. These will be referred to in the text by their paper number, written with the Roman numerals **I-III**.

I **Ko D.**, Lee J., Patel H.A., Jakobsen M.H., Hwang Y., Yavuz C.T., Hansen H.C.B., Andersen H.R. (2017). Selective removal of heavy metal ions by disulfide-linked polymer networks. *Journal of Hazardous Materials*, 332:140-148

II **Ko D.**, Kim H., Lee H., Yavuz C.T., Andersen H.R., Hwang Y. (2017). Applicability of disulfide-polymer particles surface embedded on alginate beads for cadmium removal from airport derived stormwater. *Submitted –Journal of Hazardous Materials.*

III **Ko D.**, Mines P.D., Jakobsen M.H., Yavuz C.T., Hansen H.C.B., Andersen H.R. (2017). Disulfide polymer grafted composites for heavy metal removal from stormwater runoff. *Chemical Engineering Journal (under review).*

In addition, the results of the thesis have also been presented at the following conferences during this PhD study:

Ko D., Jakobsen M.H., Hwang Y., Yavuz C.T., Andersen H.R., "Synthesis of covalent organic polymers for removing CO_2 and heavy metal ions with strong affinity," Conference proceeding, *8th Europe-Korea Conference on Science and Technology*, 108-109 (2015)

Ko D., Jakobsen M.H., Hwang Y., Yavuz C.T., Andersen H.R., "Synthesis of covalent organic polymers for removing heavy metal ions with strong affinity," Conference proceeding, *International Environmental Engineering Conference* (2015)

Ko D., Lee J., Jakobsen M.H., Hwang Y., Yavuz C.T., Andersen H.R., "Selective heavy metal capture from contaminated water," Conference Proceeding, *9th Europe-Korea Conference on Science and Technology*, 135-136 (2016)

Ko D., Lee J., Patel H.A., Jakobsen M.H., Hwang Y., Yavuz C.T., Hansen H.C.B., Andersen H.R., "Disulphide covalent organic polymers for selective removal of heavy metal ions," *3rd IWA Young Water Professionals Denmark* (2017)

Ko D., Andersen H.R., (2017), "Removal of heavy metal ions from stormwater runoff by disulphide-polymer particles surface embedded/grafted on size-tuneable support," *9th International Water and Health Seminar* (2017)

Ko D., Kim H., Yavuz C.T., Andersen H.R. and Hwang Y., "Removal of cadmium from airport-derived stormwater by disulphide-polymer particles surface embedded on alginate beads," Conference proceedings, *9th Europe-Korea Conference on Science and Technology*, 110 (2017)

Ko D., Kim H., Yavuz C.T., Andersen H.R. and Hwang Y., "Removal of cadmium from airport-derived stormwater by disulphide-polymer particles surface embedded on alginate beads," Conference Proceeding, *15th International Conference on Environmental Science and Technology*, (2017)

Acknowledgements

First of all, I would like to thank my supervisor Dr. Henrik R. Andersen for giving me the opportunity to work on this PhD project. His ambitious ideas always intrigued my questions of science, and his trust in me and my work has made this time a worthy three years. I am also grateful for the support of my co-supervisors, Dr. Yuhoon Hwang, Dr. Mogens H. Jakobsen, and Dr. Cafer T. Yavuz. I owe huge thanks to all my co-supervisors with their advice and guidance on not only the academic way but also with the wisdom of life. Special thanks to Dr. Hans Chr. Bruun Hansen for his critical advice and offering me the opportunity to collaborate with Copenhagen University. I must also say thanks to my research fellow Dr. Paul D. Mines for introducing me to the opportunity of a PhD in Denmark, a most special time in my life, with huge support.

I particularly wish to thank Sinh Hy Nguyen for always giving me instruction and help in the lab, as well as being a good lab-friend. A special thanks to Anne Harsting for supporting me throughout the whole PhD period.

Additionally, thank you to the external collaborators during my PhD project: Korea Advanced Institute of Science and Engineering (KAIST) ONE lab members, Lotte Nielsen from DTU Nanotech, Korean-Denmark Scientist Association members, fellow PhD students from Copenhagen University and students from Seoul National University of Science and Technology.

I want to thank my friends in DTU Environment for making my three years so much fun and fruitful. ENV-cake club members who gave me a feeling of sweet Friday, my dear group members Ariadni, Katie, Ravi, Kamilla, Kai, Iro, and Gordon. Special thanks to my friends who encourage me and give me big hugs: Chalotte, Biao, Yifeng, Yunjie, Carlos, Palomo, Bastiaan, Concetta. Also, I would like to thank my friends in FIBC and ShinYoung for always praying for me and sharing fellowship.

I am really grateful for my northern family Jae Seong, Hee Sup, Se Hyeuk, Tae Kwang, Yu Hoon, and Seo In. Without their support and cheers I would not have been so comfortable. Lastly, of course, to my family for their love and trust: SunMiGyeong Back, Young Hoon Ko, Dong Ju Ko, and my grandma, Gyeong Soon Kim, who had always prayed for me and is now truly resting in heaven.

Coram Deo

Summary

Numerous heavy metal removal practices for stormwater runoff have been studied and applied; however, there is still room for improvement. Among these practices, adsorption has proven to be the most efficient way of removing heavy metals. Commonly used adsorbents have an innate sorption capacity in relation to high concentrations of heavy metal ions, but if they are to be used for stormwater runoff, high affinity with rapid sorption kinetics for low concentrations of heavy metals is necessary. Therefore, in this study, new types of functional nanostructured polymer sorbents for effective heavy metal removal from stormwater are suggested.

First, comparison studies of several existing polymer sorbents were conducted, to find decisive functional groups for removing heavy metals from the solution. To enhance the sorption kinetics and affinity of polymer sorbents in the presence of competing ions, sulphur functional groups and polar functional groups in the polymer networks were found to be imperative. Based on this result, new types of covalently connected polymer sorbents were devised and characterised.

One of the novel polymer sorbents, disulphide-linked polymer (COP-63), was selected for perusing heavy metal sorption behaviour. Although COP-63 has a moderate surface area, it demonstrated cadmium removal efficiency equivalent to highly porous activated carbon (AC), while it also exhibited 16 times faster sorption kinetics compared to AC, owing to high affinity towards disulphide and thiol functionality. The chemisorption mechanism of sorbents was confirmed by sorption kinetics, the effects of pH and metal complexation. The metal ions copper, cadmium and zinc showed high binding affinity towards the polymer sorbent, even in the presence of competing cations in the form of calcium.

To retrofit polymer sorbents for a real stormwater filter, controlling the size of sorbents by formulating composites was applied. The first composites were obtained by grafting polymer onto granular-AC through acyl chlorination (DiS-AC), and the formulation of composites was confirmed by various characterisation techniques. DiS-AC demonstrated 89 L/g sorption affinity for cadmium, which is notably higher than conventional sorbents' sorption affinity. Furthermore, within an hour, half of the trace amounts of cadmium ions were removed by the DiS-AC, even in a batch test. Other composites

were obtained by embedding the polymer particles on the surface of an alginate bead (DiS-algi). Moreover, the sorption capacity of DiS-algi was 22.3 mg/g, and within 6 minutes, half of the cadmium had been removed with 31 L/mg of Langmuir sorption affinity, outperforming an AC filter.

Moreover, DiS-algi was used to build the reactive filtration column for simulating a real stormwater treatment filter. A breakthrough test of the reactive column showed the complete uptake of cadmium from a contaminated flow, lasting two hours until reaching the breakthrough point. The maximum sorption capacity of the reactive column was 877 μg/g. Furthermore, regeneration tests of the column verified its reusability.

Based on the results of this PhD, novel polymer and composites sorbents are proposed for distinct uses. The devised functional nanostructured polymers confirmed their potential for efficient heavy metal removal, and the simulation of a real-life stormwater filter was successful. Therefore, the novel polymer sorbents herein proved to be viable materials for stormwater runoff filtration systems.

Dansk sammenfatning

Talrige metoder til fjernelse af tungmetaller fra regnvandsafstrømning er blevet undersøgt og anvendt, men der er dog stadig plads til forbedringer. Blandt disse metoder har adsorption vist sig at være den mest effektive måde at fjerne tungmetaller på. Almindeligt anvendte adsorbenter har en høj sorptionskapacitet i forhold til høje koncentrationer af tungmetalioner, men hvis de skal anvendes til behandling af vand fra regnvandsafstrømning, er høj affinitet med hurtig sorptionskinetik ved lave koncentrationer af tungmetaller nødvendig. Derfor foreslås i denne Ph.D. afhandling nye typer af funktionelle nanostrukturerede polymer-sorbenter til effektiv fjernelse af tungmetaller fra stormvand.

Første blev sammenlignende undersøgelser af flere eksisterende polymersorbenter udført for at finde afgørende funktionelle grupper til fjernelse af tungmetaller fra vandig opløsning. For at forbedre sorptionskinetikken og affiniteten af polymer-sorbenter ved tilstedeværelse af konkurrerende ioner viste svovlfunktionsgrupper og polære funktionelle grupper i polymernettet at være afgørende. Baseret på dette resultat blev nye typer kovalent forbundne polymersorbenter udtænkt og karakteriseret.

En af de hidtil ukendte polymer-sorbenter, disulfidbundne polymer (COP-63), blev udvalgt til undersøgelse af tungmetal sorption. Selvom COP-63 har et moderat overfladeareal, viste det sig at cadmiumfjernelseseffektiviteten var tilsvarende den for højt porøst aktivt kul (AC). Desuden udviste COP-63 16 gange hurtigere sorptionssammenlignet med AC på grund af høj affinitet af cadmium over for disulfid og thiolfunktionalitet. Kemisorptionsmekanismen for sorbenter blev bekræftet ved sorptionskinetik, virkningerne af pH og metalkompleksdannelse. Metalionerne kobber, cadmium og zink viste høj bindingsaffinitet over for polymersorbenten, selv i tilstedeværelse af konkurrerende kationer i form af calcium.

For at kunne benytte polymer sorbenter i eksisterende regnvandsfilter, blev sorbenterne formuleret som kompositmaterialer for at opnå en passende partikelstørrelse. De første kompositter blev fremstillet ved podning af polymer på granulær AC ved acylklorering (DiS-AC), og dannelsen af kompositterne blev bekræftet ved forskellige karakteriseringsteknikker. DiS-AC demonstrerede en sorptionsaffinitet for cadmium på 89 L/g, hvilket er højere end konventionel sorbenter's sorptionsaffinitet. Desuden blev der

indenfor en time fjernet halvdelen af spormængderne af cadmiumioner, selv i batchprøver. Andre kompositter blev opnået ved at indlejre polymerpartiklerne på overfladen af alginatkugler (DiS-algi). For DiS-algi var sorptionskapaciteten 22,3 mg/g, og inden for 6 minutter blev halvdelen af cadmium fjernet med en Langmuir-sorptionsaffinitet på 31 L/mg, hvilket overgår AC.

DiS-algi blev desuden brugt til at opbygge en reaktiv filtreringskolonne for at simulere et regnvandsbehandlingsfilter. En gennembrudstest af den reaktive kolonne viste fuldstændig optagelse af cadmium fra en kontamineret vandstrøm i to timer indtil gennembrud skete. Den maksimale sorptionskapacitet af den reaktive søjle var 877 µg/g. Endvidere bekræftede regenerering af kolonnen dens genanvendelighed.

Baseret på resultaterne opnået i løbet af denne ph.d., foreslås nye polymer sorbenter til forskellige anvendelser. De udviklet funktionelle nanostrukturerede polymerer bekræftede deres potentiale for effektiv fjernelse af tungmetaller, og simuleringen af et virkelige regnvandsfilter var vellykket. Derfor viste de hidtil ukendte polymer-sorbenter heri at være realistiske materialer til regnvandsafstrømnings filtersystemer.

Table of contents

Abbreviations

AC	Activated carbon
BET	Brunauer-Emmett-Teller method
COP	Covalent organic polymer
DiS-AC	Sulphur polymer grafted activated carbon
DiS-algi	Disulphide polymer embedded alginate bead
EA	Elemental analysis
FT-IR	Fourier transform infrared spectroscopy
GAC	Granular-activated carbon
HSAB	Hard-soft acid and base
HDD	Hydrodynamic diameters
IR	Infrared spectroscopy
LOD	Limit of detection
NTA	Nitrilotriacetic acid
PE	Polyethylene
SEM	Scanning electron microscopy
TGA	Thermogravimetric analysis
WQS	Water quality standard
XPS	X-ray photoelectron spectroscopy

1 Introduction

1.1 Research background and aim

Climate change has created scattered rainfall events across the globe along with increasing problems of stormwater runoff. Localised downpours cause drainage overflows and lead to the overloading of water treatment systems. Moreover, a wide range of pollutants is flushed through by stormwater runoff, therefore increasing risk to recipients such as streams and rivers. Thus, stormwater runoff is considered as wastewater by EU legislation (Cederkvist et al. 2016).

Among the pollutants in stormwater runoff, heavy metal contamination is a notable problem for both urban and agricultural areas. Heavy metal contamination frequently exceeds water quality standard (WQS) values (Göbel et al. 2007; Fletcher et al. 2004; Pitt et al. 2004), and in urban areas, a lack of natural filtration, due to the coverage of cement, flushes a considerable amount of washed road dust (including lead, copper, cadmium, zinc, nickel, etc.) directly into streams (Yang & Toor 2017; Gittleman et al. 2017). Furthermore, atmospheric deposits aggravate heavy metal contamination during rainfall events (Sabin et al. 2005), and agricultural runoff results in noticeable heavy metal pollution derived mainly by phosphate fertiliser contamination (Azzi et al. 2017).

However, stormwater runoff treatment is still limited, due to its uncertain and dynamic nature. Among recent stormwater treatment practices, wet detention ponds, filtration and underground catchment basin insertions are the most widely used. Wet detention ponds provide a long hydraulic retention time to runoff by storing flow during a storm event and then releasing it slowly thereafter (Schwartz et al. 2017). However, due to spatial limits, catchment basin and filtration systems are commonly used in urban areas. These practices involve various mechanisms; however, for heavy metal removal, adsorption has proven to be a better technique compared to other mechanisms for the efficient treatment of stormwater runoff (Roy & Bhattacharya 2013; Crini 2005). Likewise, adsorption means low investment costs, due to the ability to treat large volumes of runoff within a short time period (Wan Ngah & Hanafiah 2008).

The most commonly used sorbents for the adsorption of heavy metal are sand, zeolite and activated carbon (Sansalone 1999), though the applicability of these sorbents is limited when treatment procedures require the instant and highly efficient removal of pollutants. Recently, various advanced materials have been proposed as efficient sorbents containing high porosity and specific functional groups (Xu et al. 2005; McDonald et al. 2012; Byun et al. 2017; Lu et al. 2012). Due to the extraordinary robustness and stability of their structure, covalent

organic polymers (COPs) have been studied extensively, among other sorbents, for targeting various environmental applications, namely gas capture (Patel & Yavuz 2015), solvent uptake (Patel et al. 2014) and groundwater remediation (Mines et al. 2016). COPs are simply obtained by forming covalent bonds between monomers in mild one-pot synthesis, and so diverse COPs can be designed by using different monomers.

In this thesis, the aim is to suggest efficient COPs sorbents for stormwater runoff that have high selectivity, rapid sorption kinetics and sufficient sorption capacity. Moreover, the suggested adsorbent is optimised in relation to its sorption function by conducting several tests. Finally, the polymer sorbent is formulated into a composite for retrofitting in a stormwater filter.

The schematic below provides an overview of the research that follows (Figure 1.1):

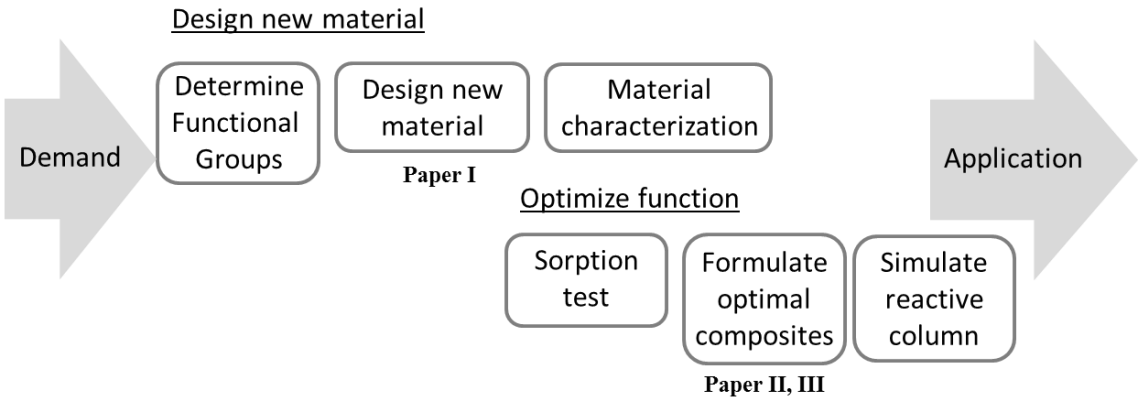

Figure 1.1 Overview of the research approach in this thesis

The objectives of the thesis are to:

- Determine the important functional groups in polymer sorbent for heavy metal removal application, by conducting comparison tests on existing polymer sorbents.
- Design a functionalised polymer sorbent to achieve efficient heavy metal removal **(Paper I)**.
- Scrutinise sorption behaviours, i.e. isotherms, kinetics, and sorption selectivity of the suggested polymer sorbent **(Paper I)**.
- Optimise the size of the polymer sorbent by formulating composites without losing sorption properties and simulating a stormwater filter with a reactive column **(Papers II and III)**.

1.2 Materials overview

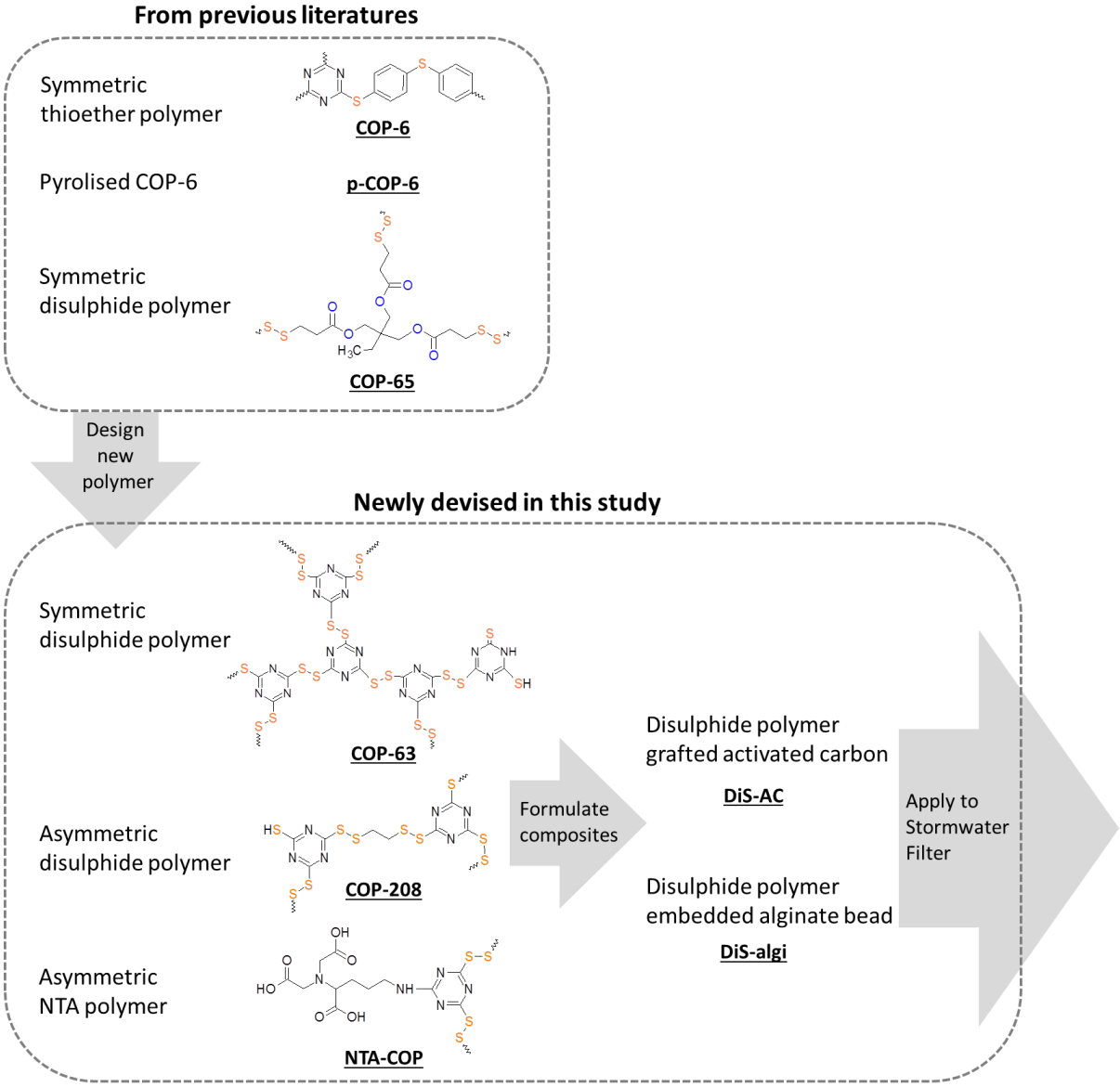

Figure 1.2 Overview of polymer sorbents and composites used in this thesis

1.2.1 Polymer sorbents from previous literatures

Three types of existing polymer sorbents were selected to find decisive functionalities for heavy metal sorbents. Symmetric thioether polymer (COP-6) and pyrolised COP-6 (p-COP-6) were compared to see the effect of surface area and sulfur functionality. Afterwards, Symmetric disulphide polymer (COP-65) was compared with COP-6 to confirm the importance of hydrophilicity of polymer.

1.2.2 Novel polymer sorbents and their composites

Brand new polymer sorbents were devised based on the result from comparison tests of existing polymers. First, symmetric disulphide polymer with hydrophilic groups (COP-63) was synthesized. Second, asymmetric disulphide polymer (COP-

208) was introduced to increase sulfur contents in the structure. Third, asymmetric disulphide polymer with nitrilotriacetic acid moieties was proposed for specific metal capture. Afterwards, two types of composites, DiS-AC and DiS-algi, were suggested to achieve the optimal grain size of filter.

1.3 Thesis structure

Chapter 2 includes studies defining the important functional groups that determine a heavy metal sorbent, which were conducted by comparing existing polymer sorbents. Based on these studies, new types of porous polymer sorbents are suggested.

In Chapter 3, the adsorption behaviour of selected polymer sorbents is scrutinised. First, sorption isotherm models are fitted onto experimental data, and other important parameters are calculated based on the isotherm. Second, the sorption kinetics of polymer networks are determined with pseudo first-order kinetics and pseudo second-order kinetics models. Lastly, the effects of pH on sorption and sorption selectivity in the presence of other competitive ions are studied.

Chapter 4 involves size engineering the polymer networks to be retrofitted into the real stormwater treatment filter. Two methods are applied in this study. First, the chemical attachment of polymer onto a carbon substrate is studied by using the acyl chlorination surface modification method. Second, the polymer networks are embedded on the surface of a coarse substrate and formulating a proper size for the filter material, without losing sorption properties. Additionally with the composites, a reactive column test is conducted to simulate a real stormwater filter.

2 Design and synthesise functionalised polymer networks

The aim of this chapter is to find appropriate functionalised nanostructured polymers for remediating heavy metal pollution from stormwater runoff. In order to be used in a real stormwater filter, rapid sorption kinetics and selectivity are important parameters, as well as sufficient sorption capacity, which is the amount of pollutant that can be captured and possessed in a gram of adsorbent. Generally, high sorption capacity is expected for an adsorbent with a high surface area. Consequently, granular-activated carbon, sand and zeolites with high surface areas are commonly used as filter materials (Roy & Bhattacharya 2013). However, commercialised adsorbents have limited uses, due to low selectivity in relation to target pollutants and slow kinetics, even though they have sufficient surface area (Sancey et al. 2011). Sorption kinetics and selectivity could be improved by enhancing the chemical adsorption properties of a sorbent, determined by functionality in the polymer networks. Therefore, in this chapter, the important functional groups for heavy metal removal were found by comparing several polymer adsorbents. Based on this knowledge, new polymer sorbents for stormwater runoff treatment are designed and synthesised.

2.1 Effect of sulphur functionality in the polymer

Sulphur functional groups were selected based on hard-soft acid and base (HSAB) theory, according to which, soft acids react preferentially with soft bases and hard acids with hard bases. This has been proven over a few decades, and so it is commonly used to explain the stability of compounds, reaction mechanisms and pathways (LoPachin et al. 2012). Since heavy metals are well-known soft acids, the soft bases, such as thiols, sulphides, disulphides and cyanides, will preferentially bind heavy metals (Ho 1975). To confirm the effect of sulphur containing functional groups, two types of polymer sorbents are compared herein. During this study, thioether polymer was selected and compared with the polymer, which had a higher surface area but less sulphur.

2.1.1 Synthesis and characterisation of thioether polymer networks (COP-6)

A one-pot synthesis method involving cyanuric chloride and 4,4’-thiobisbenzenethiol, reported by Hasmukh (Patel et al. 2013), was used to obtain the thioether polymer (Figure 2.1; COP-6).

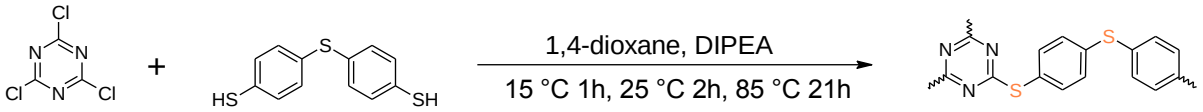

Figure 2.1 Polymerisation scheme of the thioether polymer COP-6.

The structure of COP-6 was confirmed by IR and the surface area measured by applying the physical adsorption method (Figure 2.2). Strong peaks were obtained in the 1200–1600 cm^{-1} region, showing the CN heterocycles in the triazine groups, and thioethers were spotted in the 750–600 cm^{-1} region with small peaks.

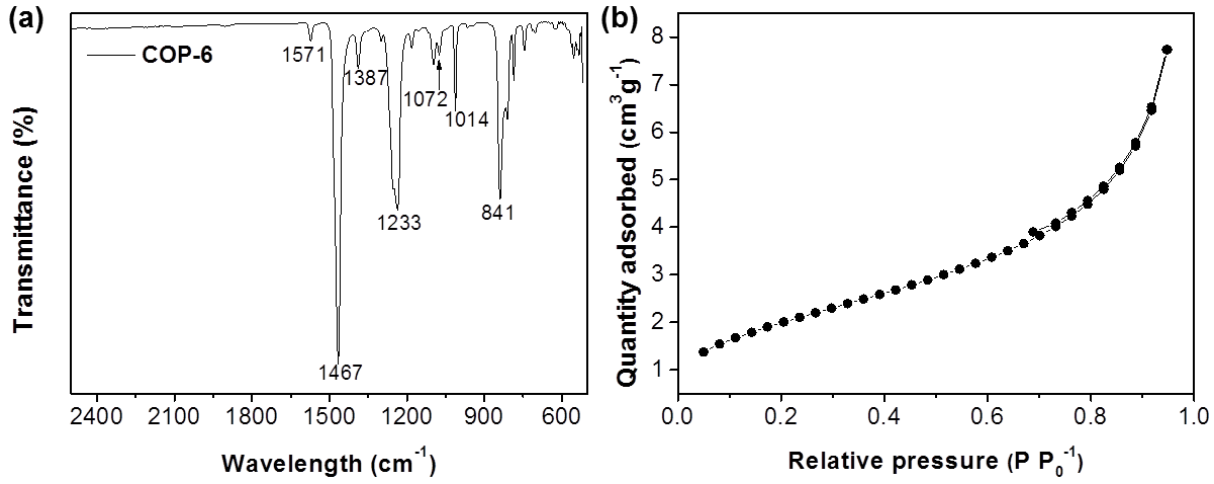

Figure 2.2 Characterisations of COP-6. (a) The IR spectrum has strong peaks in the region 1200–1600 cm^{-1}, which correspond to the CN heterocycles. Small peaks in the 600–750 cm^{-1} region show the C-S bonds. (b) The N_2 adsorption-desorption isotherm is measured at 77 K.

From Figure 2.2b, the polymer had a surface area of 7 m^2/g. Moreover, 33% of the sulphur weight was found in the COP-6 structure through elemental analysis.

2.1.2 Preparation and characterisation of pyrolised thioether polymer (p-COP-6)

As a comparison sorbent, pyrolised COP-6 (p-COP-6) was prepared through the following steps. First, the COP-6 was dispersed into a solution of potassium hydroxide and stirred for 24 hours, following which the solution was evaporated and then the remaining solids pyrolised for 3 hours at 700 ^oC, heated at a speed of 2 ^oC/min with a nitrogen flow of 200 mL/min. Lastly, the p-COP-6 was washed thoroughly with distilled water to neutralise the pH of the remaining solid. The obtained surface area of the p-COP-6 was 503 m^2/g, which is 72 times higher than the original COP-6 polymer (Figure 2.3b). In the IR spectrum, only a few peaks remained, as evidenced in Figure 2.3a, due to functional group loss during pyrolysis. Moreover, a decrease in the percentage of sulphur weight in the polymer was also observed in elemental analysis, resulting in 20% sulphur in the structure.

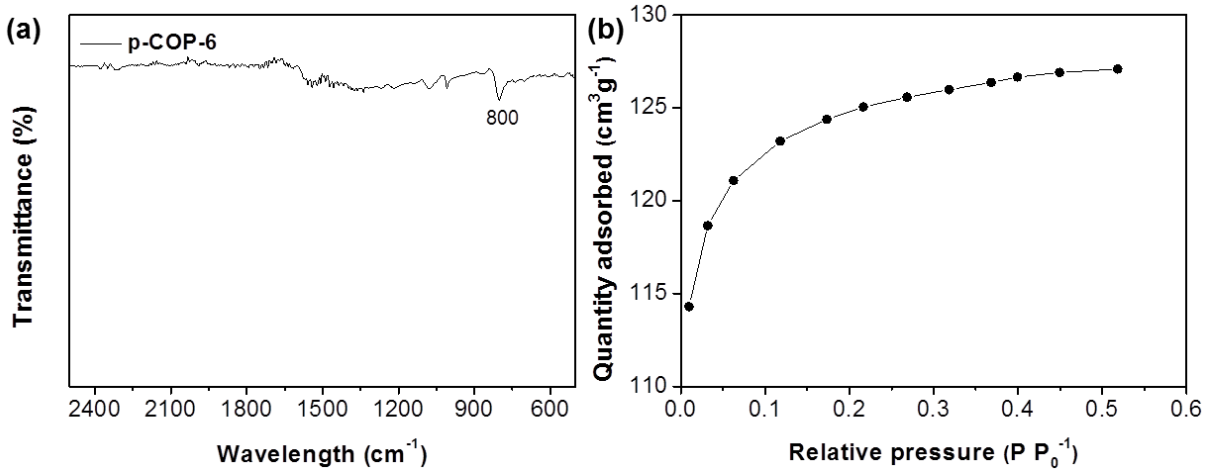

Figure 2.3 (a) The IR spectrum of p-COP-6. Most of the peaks disappeared, due to pyrolysis. The weak peak at 800 cm^{-1} represents the triazine peak. (b) The N_2 adsorption-desorption isotherm measured at 77 K.

2.1.3 Sorption comparison test

The cadmium adsorption tests for comparing COP-6 and p-COP-6 were conducted at pH 6-7 with an initial concentration of cadmium at 7.5 mg/L (Figure 2.4). During the test, p-COP-6 was highly hydrophobic, so it was difficult to ensure even dispersion throughout the solution; hence, an ethanol pre-treatment step was added, in order to run another sorption test on p-COP-6 (p-COP-6E).

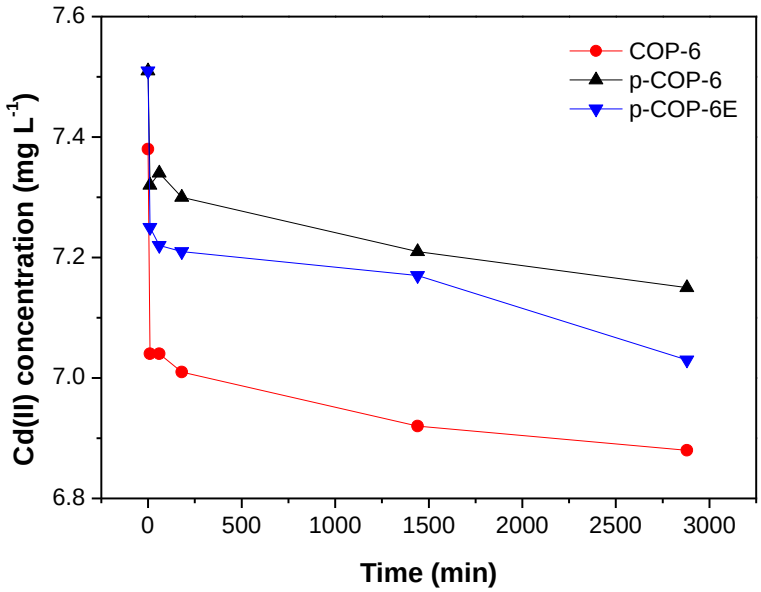

Figure 2.4 Cadmium sorption study of COP-6, p-COP-6 and p-COP-6 with an ethanol pre-treatment (p-COP-6E). Initial cadmium concentration was 7.5 mg/L, and pH was controlled in the range pH 6-7.

From the sorption test, COP-6 removed 13% of cadmium in the solution, while the p-COP-6 removed 4%. By adding an ethanol pre-treatment procedure to p-COP-6, the removal percentage improved by 2%. From this comparison study, it is evident

that even with a sorbent with a large surface areas, the percentage of sulphur functionality is a limiting factor in removal efficiency. In addition, the hydrophobicity of polymer repulses water away from the polymer, thus negatively influencing the sorption ability of the polymer.

2.2 Effect of polar functionality in the polymer

The sulphur functional group study showed that hydrophilicity is also crucial for using a sorbent in a solution. Therefore, in this study, COP-6 was compared with a disulphide polymer (COP-65), the latter of which has innate hydrophilicity, owing to its polar functional groups.

2.2.1 Synthesis and characterisation of disulphide polymer (COP-65)

Polymer hydrophilicity can be achieved by adding polar or charged groups into the structure (Lai et al. 2006). Consequently, disulphide polymer, which contains polar functionality, carboxylate ester and sulphur functional groups (COP-65) is synthesised. Due to the innate hydrophilicity, COP-65 has been shown the swelling properties on many different solvents in other study. This polymer is acquired through simple oxidative cross-linking polymerisation from one monomer, namely trimethylolpropane tris (3-mercaptopropionate), by only applying mild 80 ^{o}C heat in a dimethyl sulfoxide solution (Patel et al. 2014).

Figure 2.5 Polymerisation scheme of disulphide polymer, COP-65.

COP-65 was synthesised by following the scheme in Figure 2.5, and characterisations were conducted. As shown in Figure 2.6a, the IR spectrum confirms the formation of a disulphide linkage after polymerisation. The strong peaks at 1727 and 1130 cm^{-1} represent the carbon and oxygen double bond and single bond, respectively. The sulphur linkage is evident at 665 cm^{-1}. More sulfur related peaks generally appear below 600 cm^{-1} region, however due to the noise of the spectroscopy, below 600 cm^{-1} couldn't be measured during the comparison study. Instead, the polymer formation was cross-checked by other characterisation techniques.

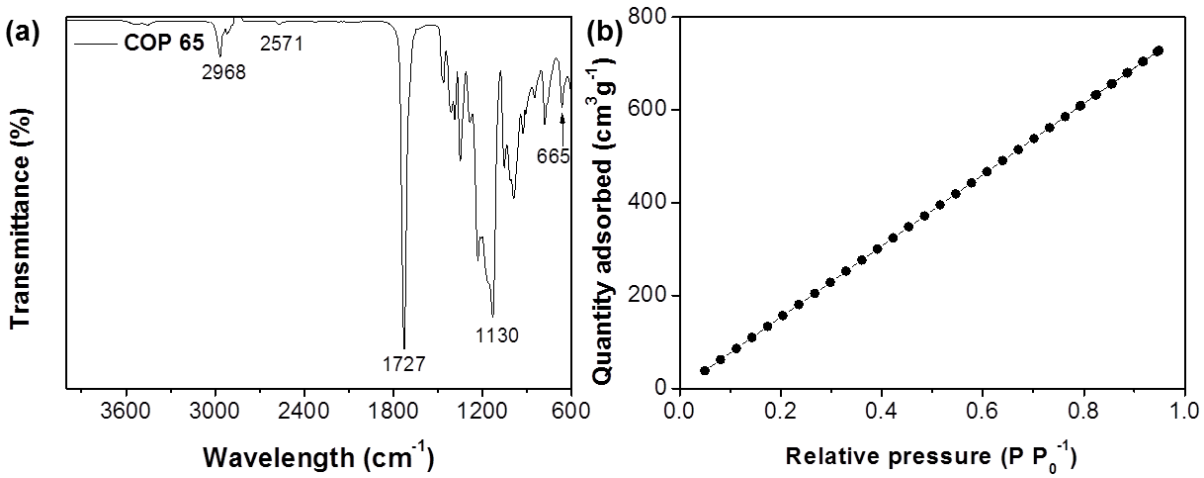

Figure 2.6 (a) IR spectrum of COP-65. The strong peaks in the 1130–1727 cm^{-1} region correspond to the C-O and C=O bonds. The small peak at 665 cm^{-1} shows the C-S bonds. (b) The N_2 adsorption isotherm measured at 77 K.

The surface area analysis (Figure. 2.6b) results in a Type III sorption isotherm, which indicates the polymer is non-porous (Fang et al. 2010), which is very much in accordance with the calculated BET surface area result of 0.0012 m^2/g. An elemental analysis was also conducted, resulting in 24% of sulphur in the structure.

2.2.2 Sorption comparison test

The sorption comparison tests were conducted at two different initial cadmium concentrations, namely 0.7 and 7.5 mg/L.

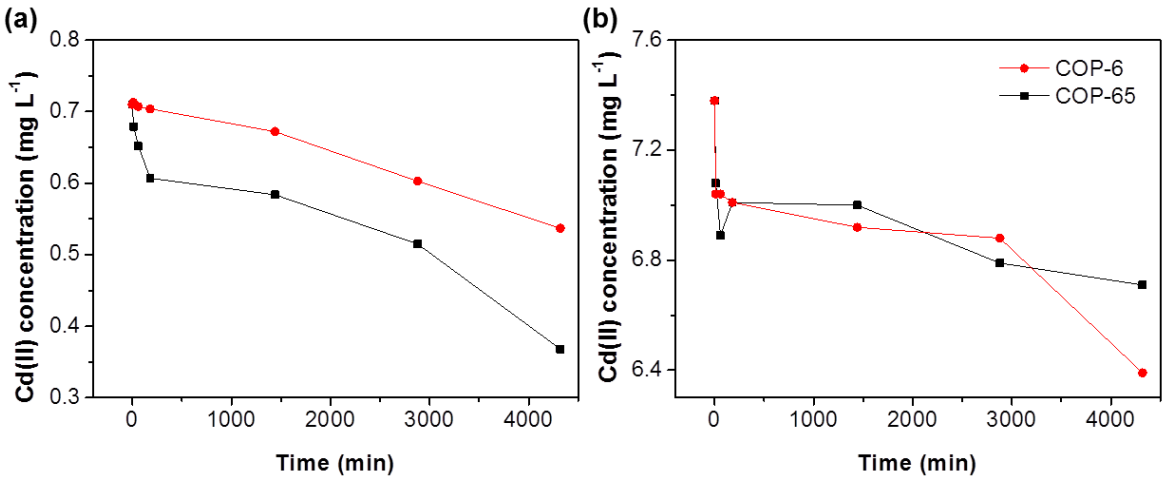

Figure 2.7 A comparison of cadmium sorption kinetic tests of COP-6 and COP-65. Initial cadmium concentrations were (a) 0.7 mg/L and (b) 7.5 mg/L.

As illustrated in Figure 2.7a, the sorption behaviours of COP-65 were more efficient than COP-6 in terms of sorption kinetics and removal percentage. The COP-65 shows 48% removal after 48 hours of contact time, while COP-6 shows 24%. However, when the higher concentration of cadmium was applied to the sorption test, COP-6 had a better removal percentage compared to COP-65, due to

the slightly larger surface area. Since COP-65 is non-porous, cadmium adsorption on the polymer was inhibited. The result of this study shows that hydrophilicity – owing to the polar functional groups – enhances sorption kinetics and removal efficiency. However, maximum capacity is related more closely to the size of the polymer's surface area.

2.3 Optimised polymer structure design

In the previous sections, the importance of sulphur and the polar functional groups was demonstrated, while a sufficient surface area was identified as being necessary for heavy metal polymer sorbents. As a result, in this chapter, new types of porous polymers are designed and suggested.

2.3.1 Symmetric disulphide polymer (COP-63)

A new polymer sorbent, which contains disulphide linkages and dangling thiols on polymer networks, is designed in this section. In addition, amines in the structure are added to introduce hydrophilicity to the polymer networks. Owing to aromatic rings in the structure, a high surface area is expected (Figure 2.8).

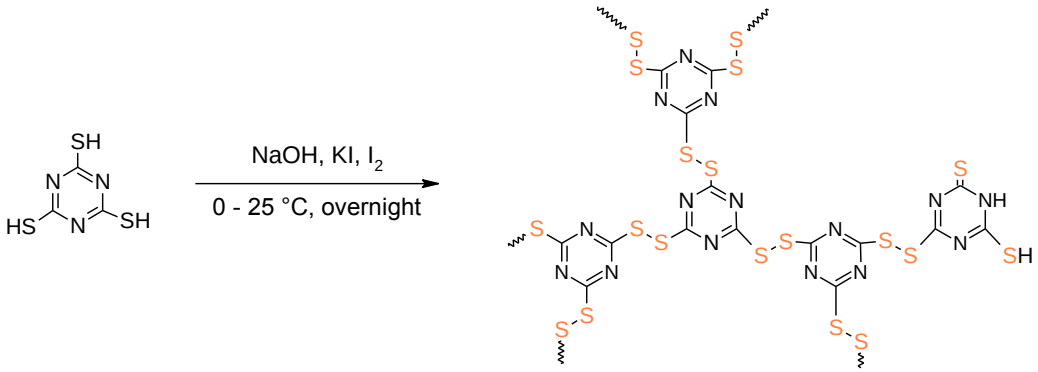

Figure 2.8 Polymerisation scheme of a disulphide linked polymer, COP-63.

Through the oxidation of thiols in the thiocyanuric acids, the monomers were linked together by a disulphide linkage, and thiols not involved in oxidation remained as dangling thiols, in order to attract heavy metal ions in the solution. This polymer was named 'COP-63' according to the COP Library naming sequence. The formation of COP-63 was confirmed by an IR spectrometer, elemental analysis and a BET surface area analyser. In Figure 2.9, the IR spectra of the monomer show N-H stretching peaks in the range 2899–3136, cm^{-1} and these peaks deteriorate in the IR spectra of COP-63. In addition, non-aromatic thione heterocycle stretching peaks, shown at 1524, 1109 and 742 cm^{-1}, shift to aromatic trithiol stretching peaks of 1466, 1230 and 825 cm^{-1}, which indicates successful polymerisation (Patel et al. 2014; Zhang et al. 2011). C=S stretching is observed at 1109 and 1119 cm^{-1} in the monomer and COP-63, respectively.

Disulphide linkages are confirmed by peaks ranging between 460 and 540 cm^{-1} (Rao et al. 1964). Lastly, the substitution of thiol sites to disulphide is confirmed by the absence of sharp S-H peaks (Tingaut et al. 2011) at 2500–2660 cm^{-1} and 1109 cm^{-1} in the COP-63 however, the remaining thione could be observed at 1119 cm^{-1} (Zhang et al. 2011).

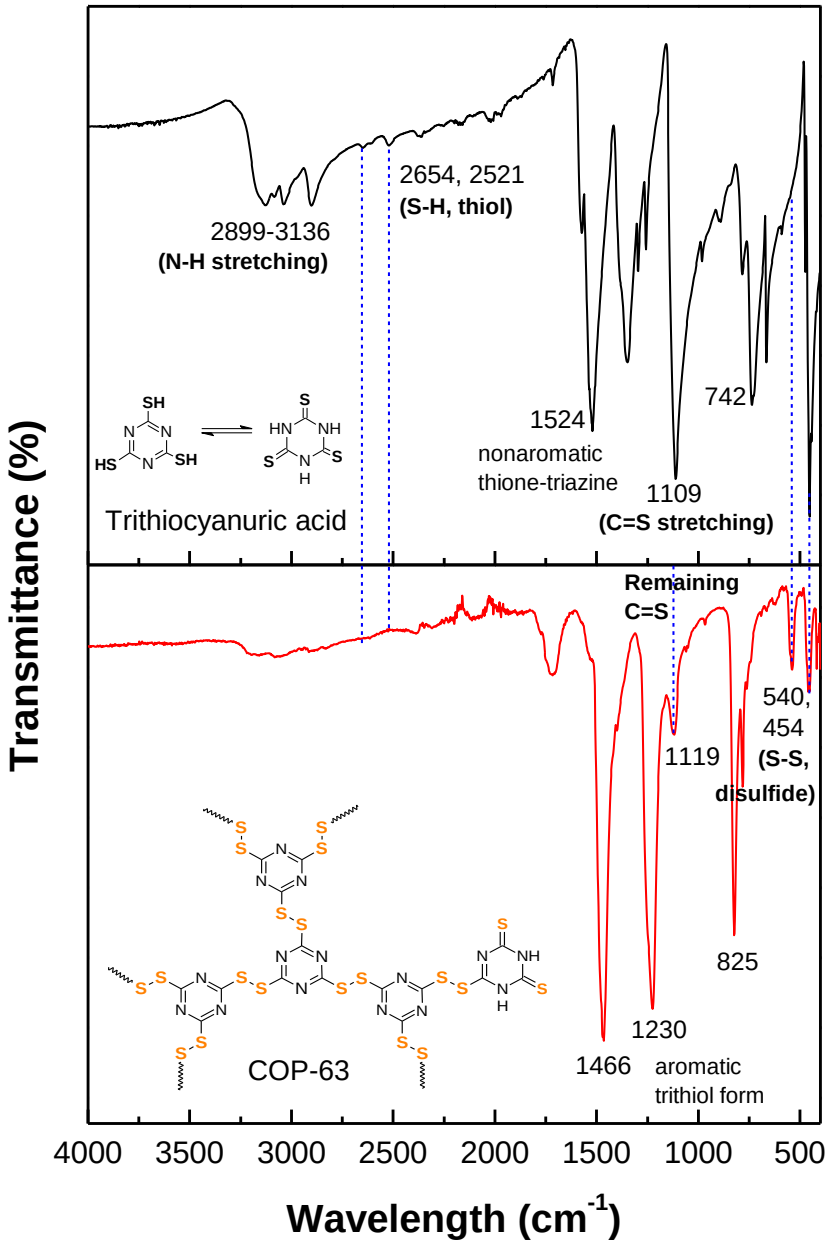

Figure 2.9 IR spectra of trithiocyanuric acid (black) and COP-63 (red). Distinctive absorption bands showed at 2899–3136 cm^{-1} (N-H, amine), 2500–2660 cm^{-1} (S-H, thiol), 700–1600 cm^{-1} (non-aromatic thione heterocycle), 800–1500 cm^{-1} (aromatic trithiol heterocycle), 1109 and 1119 cm^{-1} (C=S, thione) and 460–540 cm^{-1} (S-S, disulphide) (Paper I).

From the surface area analyser, a BET surface area for the COP-63 is calculated at 150 m^2/g. Moreover, the elemental analysis highlights that the COP-63 consists of 52.5% S, 21.3% N, 19.8% C, 0.4% H and 4.0% O, which are comparable fractions

along with the theoretical elemental percentage of COP-63: 0.46 mol of H_2O (Theoretical S: 52.7%, N: 23.0%, C: 19.7%, H: 0.5% and 4.0% O). Therefore, the formation of COP-63 functionalised by sulphur groups, as well as a sufficient surface area with hydrophilicity due to the polarity of amine in the structure, is confirmed.

2.3.2 Asymmetric disulphide polymer (COP-208)

As mentioned in previous studies, the sulphur ratio in polymer networks plays a major role in heavy metal uptake. Therefore, to increase sulphur content, another new polymer was designed and its polymerisation scheme studied. In the previous study, COP-63 was polymerised by one monomer, thiocyanuric acid, which had the same amount of carbon, hydrogen, nitrogen and sulphur atoms [$C_3H_3N_3S_3$]. Hence, by using a simple sulphur linker between the thiocyanuric acid, the total percentage of sulphur in the polymers could be increased. Based on this idea, a new polymer was designed, as illustrated below (Figure 2.10; COP-208).

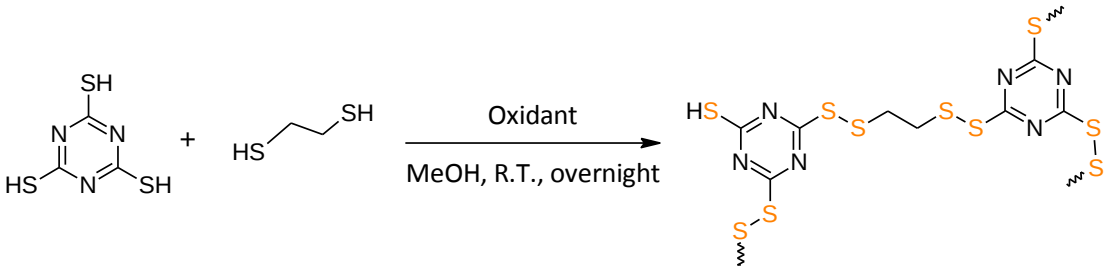

Figure 2.10 Polymerisation scheme of an asymmetric sulphur polymer, COP-208.

Polymerisation was achieved through the oxidation of thiols trithiocyanuric acid and 1,2-ethane dithiol. Even though the overall procedure is based on random polymerisation, the ratio of trithiocyanuric acid and added 1,2-ethane dithiol in this instance was 1:1.5. After overnight stirring, white precipitations were obtained, washed thoroughly and then dried at 80 ^{o}C in a vacuum. Thereafter, polymer characterisations, IR spectra and an elemental analysis were conducted.

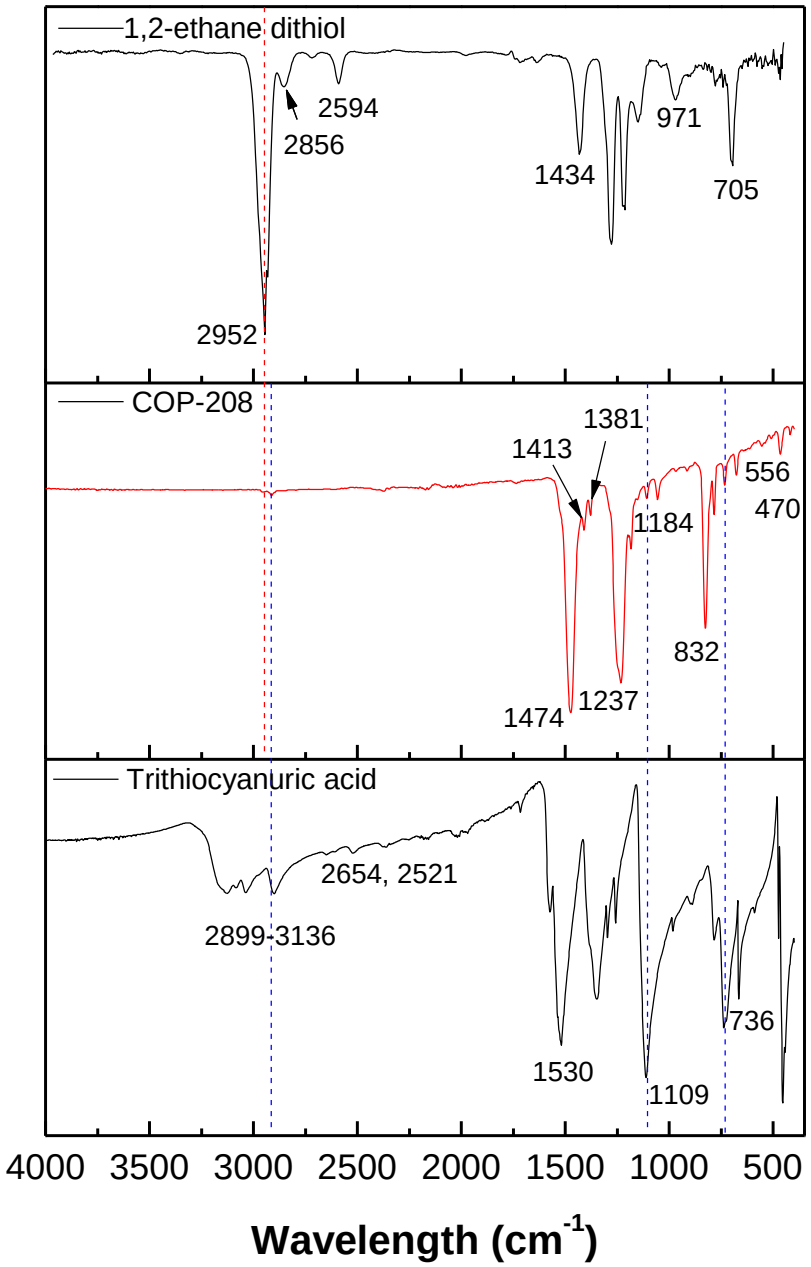

Figure 2.11 IR spectra of 1,2-ethane dithiol, COP-208 (red) and trithiocyanuric acid.

In Figure 2.11, the formation of COP-208 is confirmed by IR spectra. First, the strong peaks at 2952 cm^{-1} (C-H, alkane stretch) and 2594 cm^{-1} (S-H, thiol) in the dithiol disappear in the obtained polymer. Similarly, the distinctive peaks of thiocyanuric acid, 2899–3136 cm^{-1} (N-H, amine), 2521 and 2654 cm^{-1} (S-H, thiol) also disappear after polymerisation. Instead, at 470 and 556 cm^{-1}, disulphide bonds appear, and the non-aromatic thione heterocycle peaks at 700–1600 cm^{-1} shift to an aromatic trithiol heterocycle at 800–1500 cm^{-1}. Due to the dangling thiol on the edge of the polymer, the remaining thione (C=S) peak is observed at 1184 cm^{-1}. The results of the elemental analysis show that COP-208 consists of 60.6% S, 12.2% N, 24.0% C, 2.3% H and 1.0% O, which are comparable fractions

with the theoretical elemental percentage of COP-208, assuming that all monomers have been consumed (Theoretical S: 62.1%, N: 13.3%, C: 22.8%, H: 2.9% and 0% O).

2.3.3 Nitrilotriacetic acid containing polymer (NTA-COP)

In this last section, a polymer is designed specifically for the removal of nickel by using nitrilotriacetic acid (NTA), which has strong affinity with coordinating nickel bonds (Lauer & Nolan 2002). In order to obtain a polymer with NTA, a stepwise approach was implemented for the polymerisation scheme (Figure 2.12). First, dimers with NTA were prepared to ensure structure rigidity and to attach further polymerisation linker parts (Figure 2.12a). Second, the other monomer was added, to make NTA-COP (Figure 2.12b).

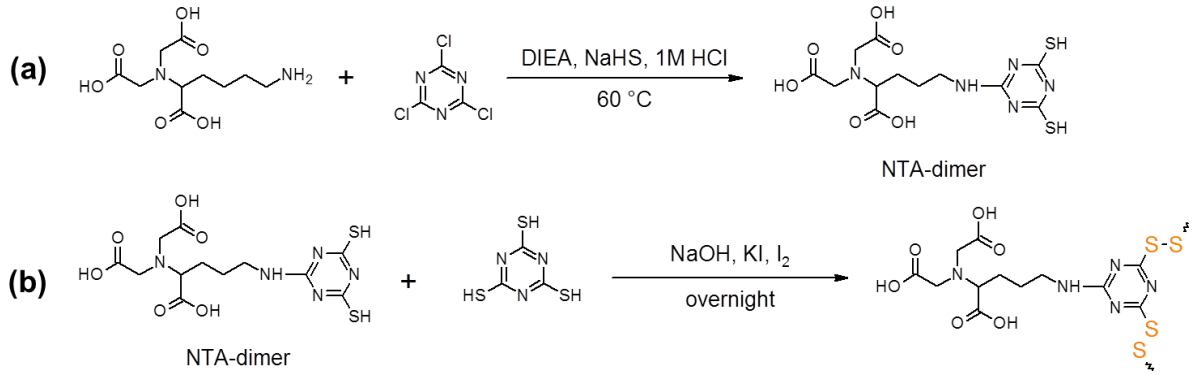

Figure 2.12 Synthesis scheme of (a) an NTA-dimer formation with NTA and cyanuric chloride and (b) the polymerisation scheme for NTA-COP.

To date, the dimerisation of model tests has been done with monomer that is simpler than NTA but contains the same active sites, i.e. 6-aminohexanoic acid. A light-brown powdery dimer was obtained during this model test. As a further study, the model test will be implemented to NTA-dimer synthesis. With an NTA-dimer, further polymerisation is attainable in relation to nickel removal.

3 Heavy metal sorption behaviour study of disulphide-linked polymer

From among the synthesised functionalised polymer networks in the previous chapter, disulphide-linked polymer (COP-63), for heavy metal removal, is selected for a sorption behaviour study. In this chapter, the sorption behaviour of a sorbent is scrutinised by applying sorption isotherms and kinetics models. To determine pH effects, the zeta potential of COP-63 is measured and sorption tests in various pH conditions are conducted. Moreover, selective interaction between heavy metal ions and COP-63 in the presence of competitive metal ions is determined. As a comparison for sorption behaviour, a common sorbent in the market, in this case activated carbon (AC), is used (Roy & Bhattacharya 2013). Figure 3.1 describes the selective sorption of heavy metal ions into COP-63.

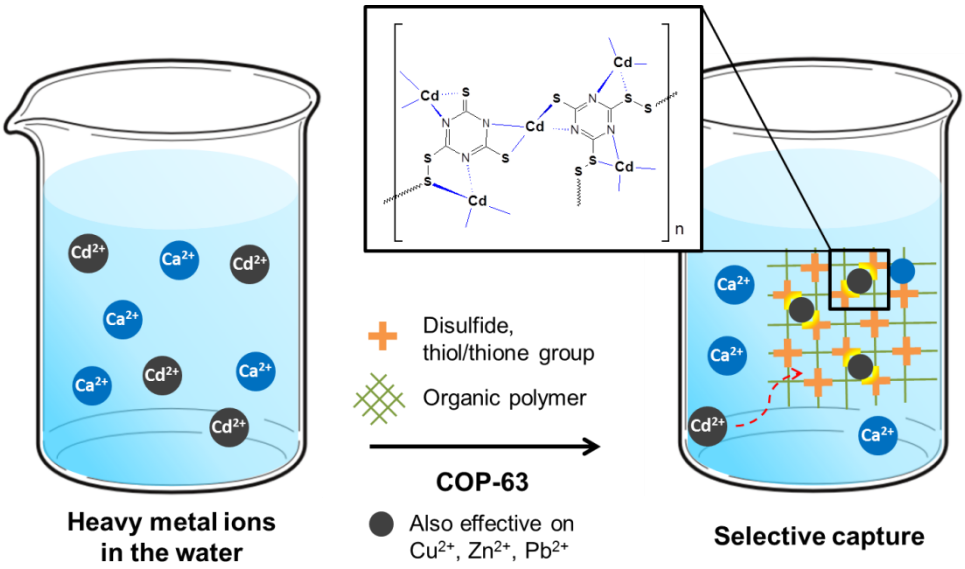

Figure 3.1 Selective interaction between heavy metal ions and sulphur functional groups in the polymer network and in the presence of competitive ions (Paper I).

3.1 Sorption isotherm study

3.1.1 Langmuir isotherm model

Sorption behaviour, based on the assumption of monolayer adsorption with a fixed number of localised sorption sites, can be explained by the Langmuir isotherm model (Foo & Hameed 2010), which describes homogeneous adsorption without any lateral interaction or steric hindrance between adsorbates, i.e. heavy metal ions. The maximum amount of heavy metal ions adsorbed into a polymer network at equilibrium (q_e) can be calculated by using the equation below (Allen et al. 2004):

$$q_e = \frac{q_m a_L C_e}{1 + a_L C_e} \quad (1)$$

where q_m is the maximum sorption capacity of the sorbent (mg/g), C_e is the equilibrium concentration of the adsorbate in solution (mg/L) and a_L is the Langmuir affinity constant (L/mg).

3.1.2 Freundlich isotherm model

The Freundlich isotherm model, on the other hand, covers the assumption behind multilayer adsorption that describes non-ideal and reversible adsorption (Allen et al. 2004). The expression can be described as follows (Hadi et al. 2015):

$$q_e = K_F C_e^{1/n} \quad (2)$$

where K_F is the Freundlich constant and 1/n is the heterogeneity factor. The Freundlich constant, K_F, is an indication of the capacity of the sorbate associated with the sorbent (Hameed et al. 2007). The heterogeneity of the sorption sites and the sorption favourability factor is determined as a value, n, which is derived from non-linear fitting. The isotherm with n > 1 indicates chemisorption with high affinity between the adsorbate and the adsorbent (Jodeh et al. 2014; Boparai et al. 2011).

3.1.3 Sorption isotherm of COP-63

To determine the heavy metal sorption affinity and capacity of COP-63, both the Langmuir and the Freundlich isotherm models were fitted on experimental data. As shown in Figure 3.2, the experimental data fitted accordingly to the Langmuir sorption model. The fitted r^2 with the Freundlich sorption isotherm, however, was lower than the Langmuir isotherm, due to the homogeneous sorption sites in both COP-63.

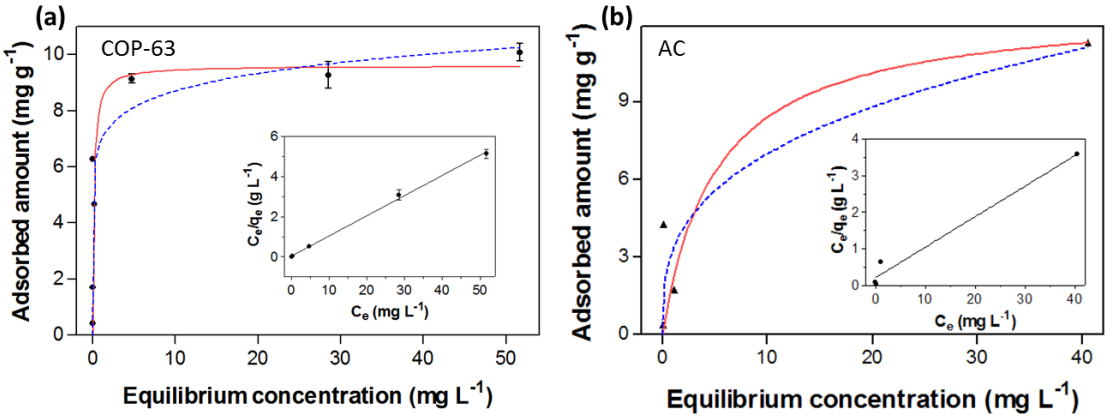

Figure 3.2 Amounts of cadmium ions adsorbed into the (a) COP-63 and (b) AC after 48 h equilibrium time at pH 6–7 in ambient conditions. Plots are fitted with the Langmuir (red, solid line) and the Freundlich (blue, dotted line) sorption isotherms. Inset: Linear

regression of the Langmuir isotherm with r^2 = 0.99 for COP-63, while r^2 = 0.98 for AC. Error bars represent a 95% confidence interval (Paper I).

The maximum sorption capacity of the COP-63 (q_m), estimated from the Langmuir isotherm linear regression, reached 9.9 mg/g, while AC was 11.9 mg/g (Figure 3.2). AC has slightly higher maximum sorption capacity; however, it is important to note that the BET surface area of COP-63 is 150 m^2/g, whereas the surface area of AC is 1,100 m^2/g. Therefore, the cadmium maximum sorption capacity per surface area of COP-63 is 0.07 mg/m^2, which is seven times higher than the capacity of AC's 0.01 mg/m^2. Moreover, the Langmuir affinity constant (a_L) of COP-63 was 3.43 L/mg compared with 0.39 L/mg for AC, illustrating that COP-63 has nearly 10 times higher sorption affinity compared to AC.

3.2 Kinetic study

Sorption kinetics is an important parameter that provides an understanding of the sorption mechanism and give insights into designing filter column (Ali & Gupta 2006). For instance, kinetics is used for determining the size of the filter that is required relative to water flow that needs to be treated. This is particularly important in the treatment of stormwater runoff, which occurs sporadically but in large volumes and therefore requires fast sorption kinetics (Field et al. 1994). To determine sorption kinetics, pseudo first-order kinetics and pseudo second-order kinetics were applied to experimental data. A pseudo first-order kinetic model is suggested by Lagergren (Abou-Gamra & Ahmed 2015), the linear form of which is formulated as:

$$\ln(q_e - q_t) = \ln q_e - k_1 t \tag{3}$$

where q_e represents the amounts of metal ions adsorbed (mg/g) at equilibrium and q_t is the amount adsorbed (mg/g) at time t. Value k_1 is the rate constant of the sorption (1/min).

Another model for describing chemisorption, provided by Ho and McKay (Ho & McKay 1999), applies pseudo second-order kinetics that can be expressed as:

$$\frac{t}{q_t} = \frac{1}{k_2 {q_e}^2} + \left(\frac{1}{q_e}\right) t \tag{4}$$

where k_2 is the rate constant (g/mg·min), while the other terms have the same meaning as Equation (3).

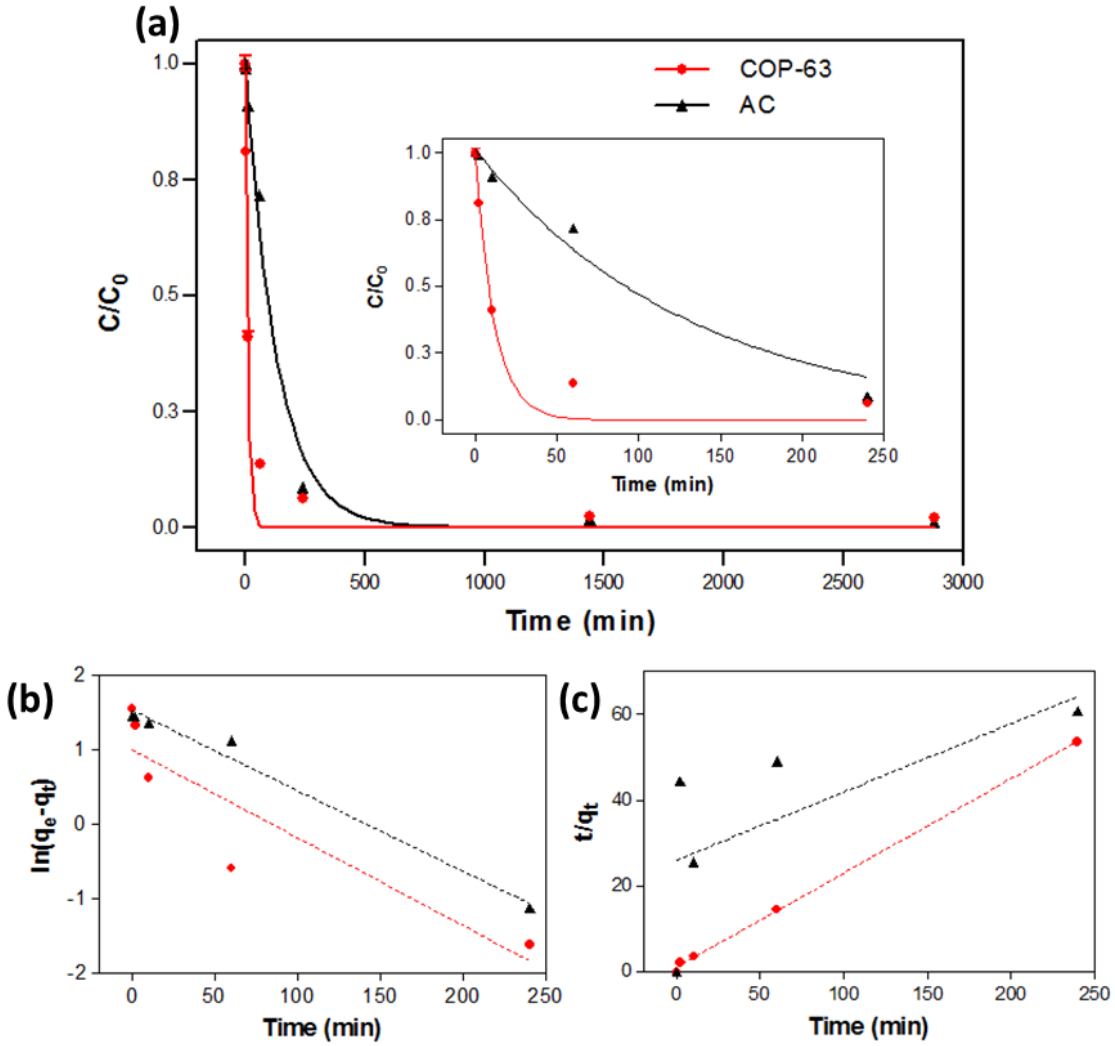

Figure 3.3 Kinetics of cadmium sorption to COP-63 and AC. (a) Cadmium removal plotted versus time and lines, due to fitting by the first-order kinetic model. Initial concentration is 10 mg/L. Error bar refers to standard deviation (n=3) Inset: Enlarged graph from initial to 240 min. (b) Pseudo first-order kinetics model fitted by linear regression for cadmium sorption on COP-63 and AC. (c) Fitting of the pseudo second-order kinetics model to sorption data (red symbols: COP-63, black symbols: AC) (Paper I).

As a result of our kinetics tests, 98% of cadmium ions were adsorbed by both sorbents, i.e. COP-63 and AC, within 3,000 min (Figure 3.3a). However, COP-63 and AC exhibited significant differences in terms of rate of sorption (Figure 3.3a, inset). To find the best-fitting kinetics model for the adsorbents, both the pseudo first-order kinetic (Eq. (3)) and the pseudo-second order kinetic models (Eq. (4)) were fitted, as illustrated in Figures 3.3b and c. By comparing model fits, the pseudo second-order kinetic model is shown to be the best fit for COP-63 (r^2 = 0.99). On the other hand, AC sorption data are better described by the pseudo first-order model (r^2 = 0.98), which may confirm the main sorption mechanisms of COP-63 with chemical sorption and AC with physical sorption to AC (Morsi & Elsabee 2015; Zhou et al. 2016). This finding is highly relevant to stormwater runoff application, because half of the cadmium is removed by AC in 63 min,

whereas the half-life for sorption by COP-63 is 4 min. Thus, filters with much lower residence times can be made by using COP-63 compared to AC, due to the much faster cadmium sorption of COP-63.

3.3 Effect of pH on polymer sorption ability

As proven in the kinetics study, the sorption behaviour of COP-63 is derived mainly by chemisorption, and so specific active sites, namely disulphide and thiol-binding sites, play a critical role in heavy metal sorption. To utilise these active sites, a negative charge on the polymer and the diffusion of metal ions to active sites are important. When the polymer surfaces are negatively charged, which can be determined by zeta potential, active binding of cations can be expected (Dai 1994; Lin et al. 2003) as well as the formation of strong covalent bonds between metal ions and the bonding sites (Zhang et al. 2008). The diffusion of metal ions to active sites can be determined by the hydrodynamic diameters (HDDs) of the COP-63 particles, which explains the aggregation of particles. Aggregation tends to increase the distance between metal ions and an active binding site, thus slowing down the sorption kinetics. To investigate the efficiency of COP-63 active sites, the zeta potential and HDDs were examined in five different pH conditions (Table 3.1).

Table 3.1 Mean value of the zeta potential (mV) and hydrodynamic diameter (HDD) (µm) of COP-63 at different pH levels (Paper I).

pH	Zeta Potential (mV) Mean values of two measurements	HDD (µm) and standard deviation
2.9	-3.4	1.5 ± 0.5
5.3	-26.8	0.4 ± 0.1
6.7	-33.45	0.3 ± 0.1
8.0	-32.1	0.3 ± 0.1
10.3	-31.1	0.4 ± 0.1

As shown in Table 3.1, the lowest zeta potential is observed at pH 6–8, ranging from -32.1 to -33.4 mV. In addition, the smallest HDD is shown in the same pH region. Based on this result, COP-63 is expected to have the highest chemisorption of heavy metal ions at pH 6–8, which aligns well with a typical stormwater runoff pH range. In the case of high pH (pH 10.3) values, COP-63 particles show a slightly weaker negative zeta potential and a higher HDD diameter, both of which are similar to the values in the pH 6–8. Hence, even at a high pH, COP-63 is expected to have similar sorption properties as at pH 6–8. On the other hand, at a low pH values below 5.3, COP-63 shows a smaller zeta potential and a significantly higher hydrodynamic diameter, which leads to the aggregation of particles and the possible slowing down of the rate of sorption (Zhang et al. 2008).

To prove the binding interaction between an active COP-63 site and heavy metal ions, in accordance with the zeta potential and HDD, five heavy metal ion adsorption tests were conducted for eight different pH values. Furthermore, each heavy metal speciation was calculated by Visual MINTEQ, following which confirmed metal-free ions and solubilised complexes were the major species in all sorption and kinetic experiments (Figure 3.4).

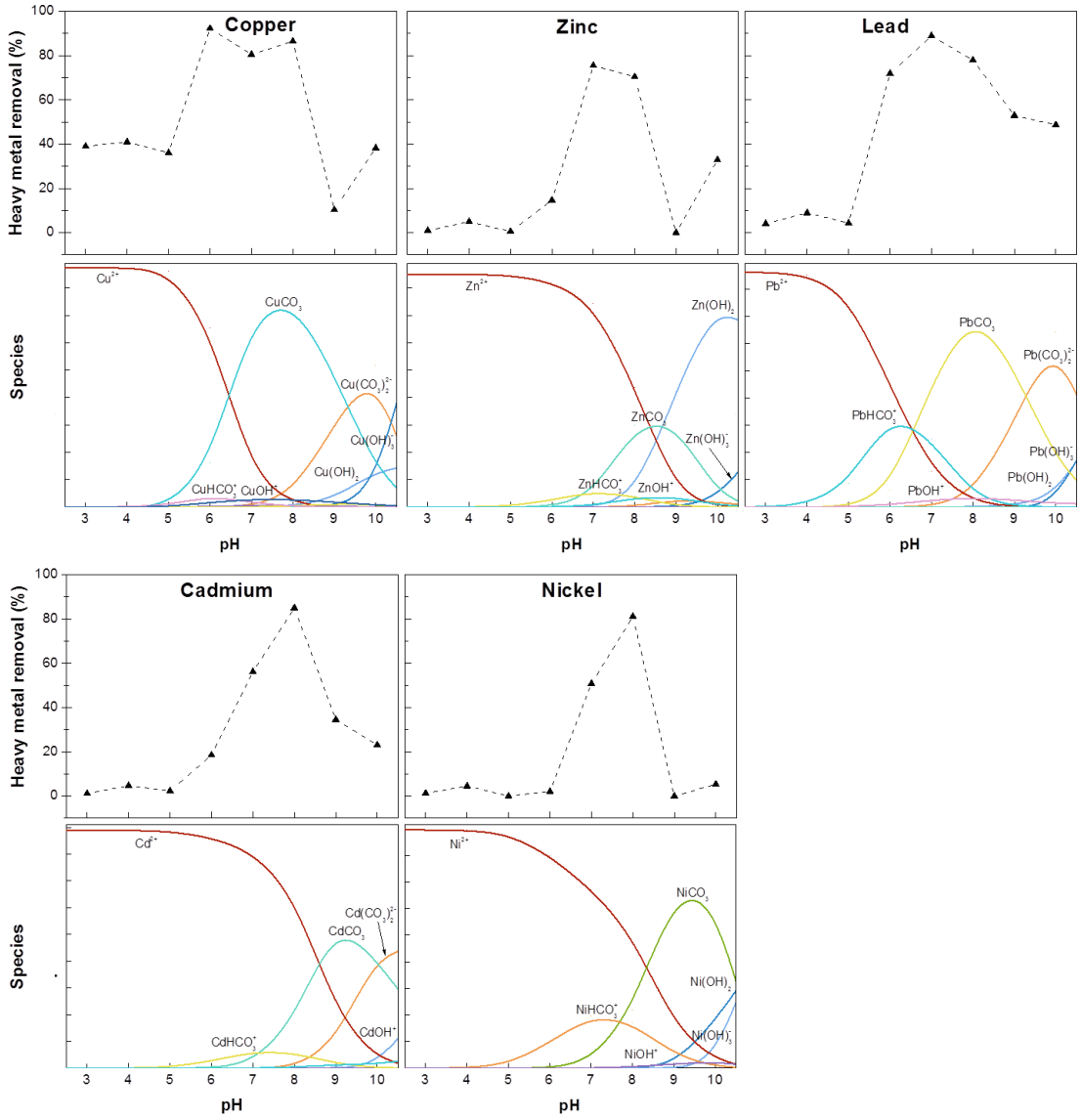

Figure 3.4 Binding interactions between COP-63 and five different heavy metal ions, namely copper, zinc, lead, cadmium and nickel, in different pH conditions. Black plot with a dashed line is the metal ion removal percentage, and coloured lines indicate speciation in each pH condition. A sorption test was conducted with 10 mg/L of initial heavy metal concentration and a dose of polymer at 0.2 g/L. The speciation of metal, including a carbonate buffer system, was calculated by Visual MINTEQ 3.0 (Paper I).

Sorption at pH 6–8 had the highest removal efficiency, as expected, based on the zeta potential and HDD values. However, when pH exceeded the range of pH 6-8,

metal ions forming negatively charged metal complexes and the complexes did not bind to negatively charged active sites in the polymer. Therefore, even though COP-63 does indeed activate sorption sites, the sorption of heavy metal ions is somewhat inauspicious. Thus, during the test, sorption at pH 10 declined, even though the zeta potential and HDD of the polymer were similar to values at pH 6-8. In the low pH region, due to the significant competition between protons and metal cations for binding sites (Genç-Fuhrman et al. 2016), the overall sorption efficiency of COP-63 decreased. Besides, a smaller zeta potential and higher HDDs could explain low sorption efficiency at low pH values.

In conclusion, the highest chemical sorption capacity appears at an intermediate pH value of 6-8, in accordance with sufficient negative fields and a high contact area on COP-63s active sites.

3.4 Role of functional groups in the polymer

The most commonly used sorbents for removing heavy metals are sand, zeolite and activated carbon (Roy & Bhattacharya 2013). However, there is a significant hindrance to removing heavy metal ions, owing to abundant competitive divalent cations such as calcium and magnesium in stormwater runoff. Hence, one of the criteria to be used in the stormwater filter is sufficient sorption selectivity in relation to the targeted metal ions. Thus, sorption studies in the presence of competitive cations were conducted, in order to determine the sorption selectivity of COP-63 regarding heavy metal ions. Five different heavy metal ions that are easily found in stormwater runoff were used, namely copper, zinc, lead, nickel and cadmium. As a competitive cation, one of the most abundant divalent cations in water, calcium, was added in different concentrations.

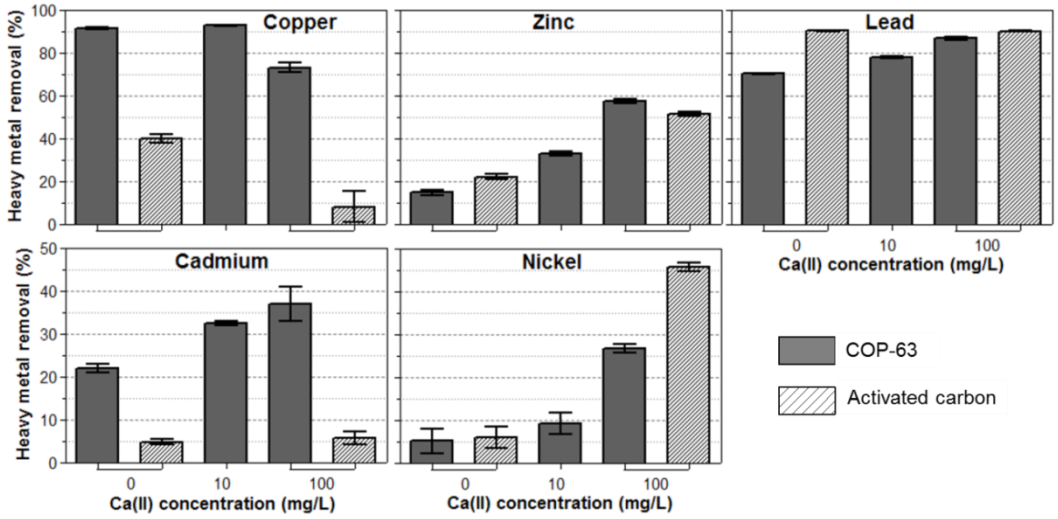

Figure 3.5 Selective sorption of five different heavy metal ions in the presence of calcium as a cation competing with COP-63 and AC. Three different concentrations of calcium ions (0, 10 and 100 mg/L) were added to heavy metal ion solutions at pH 6–7 (Initial metal

concentrations: 10 mg/L each, sorbent concentration: 0.2 g/L, contact time: 24 h). Error bars represent standard deviation (n = 3) (Paper I).

As shown in Figure 3.5, the presence of calcium has different influences on the sorption of heavy metal by COP-63 and AC. The most obvious difference in this study was shown in a copper removal test, where COP-63 had strong bonding properties in relation to copper but had only a minor effect with calcium, while the sorption of AC was hindered by calcium. In the case of other heavy metals, an increase in the concentration of calcium positively affected the adsorption of the targeted metal ions. It is important to note that for zinc and cadmium, COP-63 has greater sorption selectivity than AC in the presence of calcium. However, tests with nickel and lead demonstrated that there was less selective sorption on COP-63 compared to AC in the test conditions, because copper and cadmium are well-known soft acids and have higher polarisability, which means these metals can contribute to affinity, due to a higher tendency toward electron distortion. On the other hand, there are 'borderline acids', namely nickel, lead and zinc, that have less affinity to soft bases compared to strong soft acids (Lemire et al. 2013). Accordingly, our selectivity test established that COP-63 can selectively adsorb targeted heavy metal ions, in this case copper, cadmium and zinc, in the presence of up to a 10 times higher concentration of calcium in water. Moreover, COP-63 demonstrated an excellent ability to sorb cadmium from water, as K_d reached 4.29 x 10^5 L/kg at the equilibrium concentration of 1 µg/L. Based on a recent study (Shin et al. 2007), a K_d value of 10^4 L/kg is considered quite good, and a K_d value of 10^5 L/kg is considered excellent.

4 Formulation of material for real water treatment application

To retrofit the stormwater filtration system, the filter material should meet certain size criteria. The previous chapters focused on fundamental studies of adsorption behaviour, depending on properties of the polymer networks and the chemical effects of functional groups. The devised polymer adsorbents in Chapter 2 were generally obtained in a powdery form smaller than 50 µm; however, in order to meet filter material size criteria, the adsorbent has to be at least bigger than the effective size range of the rapid flow filter grain at 0.4 to 2 mm (Chen et al. 2005). Besides, in a pilot plant study for rapid flow filtration, 0.7–1.4 mm grains were used (Van der Aa et al. 2002). Thus, in this chapter, the engineering perspective will be implemented, to find a way of increasing the size of the adsorbent – without losing its sorption ability.

4.1 Polymer grafted activated carbon (DiS-AC)

Composites, sulfur polymer grafted activated carbon (DiS-AC), were obtained by grafting dangling thiol handles onto the surface of cheap and common granular-activated carbon (GAC). Composite characteristics were scrutinised in both physical and chemical ways and confirmed the successful grafting of the polymer with thiol handles. Moreover, sorption isotherms and kinetics were obtained from sorption tests in low concentrations of heavy metal. The novel composite, DiS-AC, exhibits potential as an ideal filter candidate for treating stormwater runoff flows (Figure 4.1).

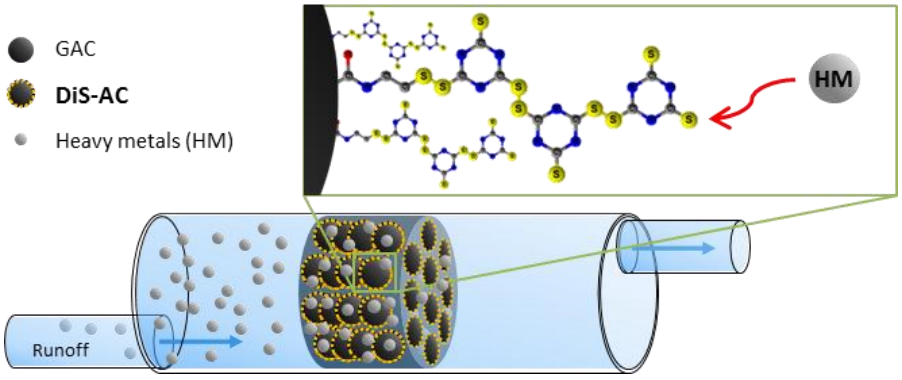

Figure 4.1 Schematic of low-concentration heavy metal removal of DiS-AC composites in polluted water.

4.1.1 Preparation of DiS-AC

To synthesise the composite of DiS-AC, we followed four steps (Figure 4.2). First, raw GAC was oxidised with a mixture of HNO_3 and H_2SO_4 to form carboxyl

groups on the surface of the GAC. Next, the carboxyl groups were activated with $SOCl_2$ to form acyl chloride groups (Mines et al. 2017). On these sites, linear thiols were attached to the surface of the acyl chloride activated GAC by adding a mixture of dimethylformamide and cysteamine, in order to make a linker for further polymerisation. The last step involved the polymerisation of thiocyanuric acid with thiol linkers on the GAC, following which a polymer-grafted GAC was obtained and dried at 80°C in a vacuum.

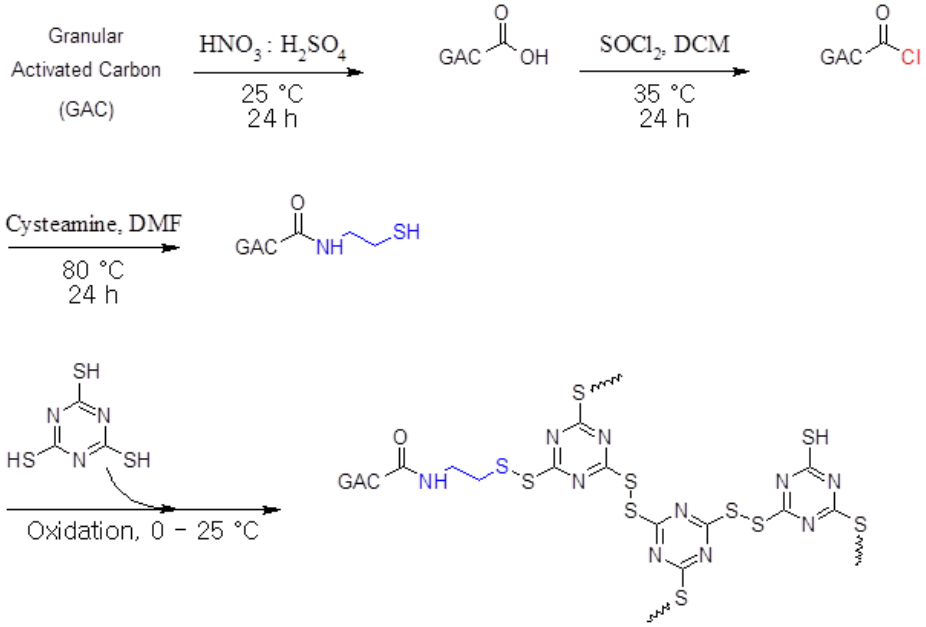

Figure 4.2 Step-wise procedures for DiS-AC formulation. Initially, bare GAC oxidized and modified through acyl chlorination. Afterwards, cystamine attachment conducted on the surface modified GAC. Finally, the polymer grafting has been implied on the cystamine attached GAC (Paper III).

4.1.2 Properties of DiS-AC

Various characterisation techniques were implemented, in order to determine the properties of DiS-AC. Morphology of the material was imaged by scanning electron microscopy (SEM), and the surface area was measured with a physisorption surface characterisation analyser. Chemical composition of the DiS-AC was determined by elemental analysis (EA), X-ray photoelectron spectroscopy (XPS) and thermo-gravimetric analysis with Fourier-transform infrared spectroscopy (TGA-IR). Visual evidence of the successful grafting of polymer to the surface of the GAC was observed via SEM (Figure 4.3). Figure 4.3a and b, the overview of morphology has been shown for GAC and DiS-AC, respectively. In Figure 4.3c common nature of the GAC, which contains random and amorphous porosity, was found (Bhatnagar et al. 2013). However, after carrying out the surface modification steps, many of the pores were filled in by polymers and showed a distinct nature of the surface's structure (Figure 4.3d).

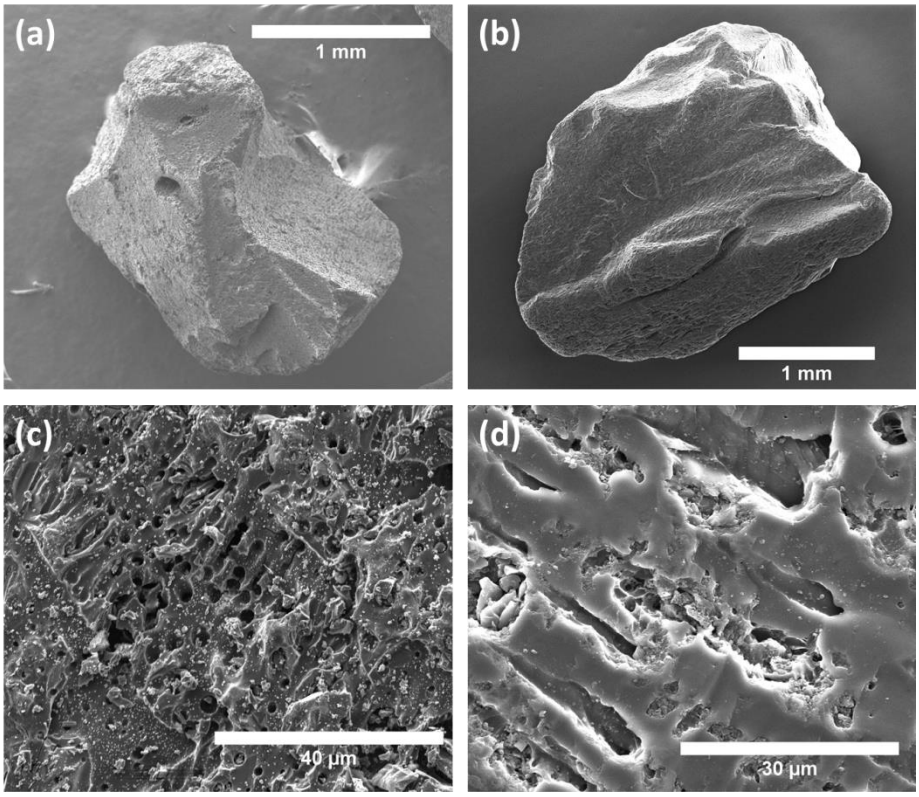

Figure 4.3 Scanning electron microscopy images of (a) overview morphology of granular-activated carbon (b) overview morphology of DiS-AC (c) granular-activated carbon surface and (d) DiS-AC surface (Paper III).

The BET surface area of DiS-AC was 674 m^2/g, while the raw GAC was 943 m^2/g, which is a slightly higher surface area compared to DiS-AC. This is the indication of infiltrating and covering polymers on raw GAC pores. However, it is important to note that although the grafted polymers filled in a noticeable amount of GAC pores, there was still quite a high surface area remaining, since the polymers also possess their own porosity. The chemical composition of DiS-AC found from the EA shows that the DiS-AC consists of 77.2% carbon, 1.5% nitrogen and 1.4% sulphur. Assuming that the repeating unit of polymer is $[C_6ON_4S_4H_5]_n$, the single GAC gained 4% in weight from the grafted polymer, which is compatible with observations made regarding weight differences measured from raw GAC and DiS-AC. Table 4.1 shows the chemical composition percentages of the different steps in the surface modification process, obtained by XPS. In the raw GAC, 92% of the material is carbon while after oxidised, 2.4% more of oxygen is shown in the result. When the linker, cysteamine (C_2H_7NS), was grafted onto the oxidised carbon substrate, 2.6% nitrogen and 0.9% sulphur appeared. Finally, the composition of DiS-AC has changed and yields 3.6% of nitrogen and 1.0% of sulphur.

Table 4.1 Atomic surface percentages of the different acyl chloride surface modification steps for GAC, as determined by XPS (Paper III).

Element	GAC	GAC-oxidised	GAC-cysteamine	DiS-AC
C	92.0	89.6	83.9	80.5
O	8.0	10.4	9.8	9.5
N	-	-	2.6	3.6
S	-	-	0.9	1.0
Other	-	-	2.9	5.3

Surface screening results for the raw GAC and DiS-AC are shown in Figures 4.4a and b, highlighting some distinct differences in the existence of nitrogen and sulphur after the polymer grafting steps. To gain further insights into the nature of the composite, an ion-etching technique with an XPS instrument was implemented. This method is based on stripping the top layers of the surface and exposing underlying components. In particular, the S2p region of sulphur is examined, and any changes in sulphur functionality throughout the layers are elucidated (Figures 4.4c and d). In Figure 4.4c, it is illustrated clearly that sulphur functionality changed as layers are etched away from the surface. The two major peaks for disulphide S-S (163.9 eV) and sulphur oxide S-O (168.4 eV), and the two secondary peaks S-C (165.4 eV) and S-H (163.2 eV), are observed on the top layers (Castner et al. 1996; Descostes et al. 2000), but these disappear when they approach the GAC substrate.

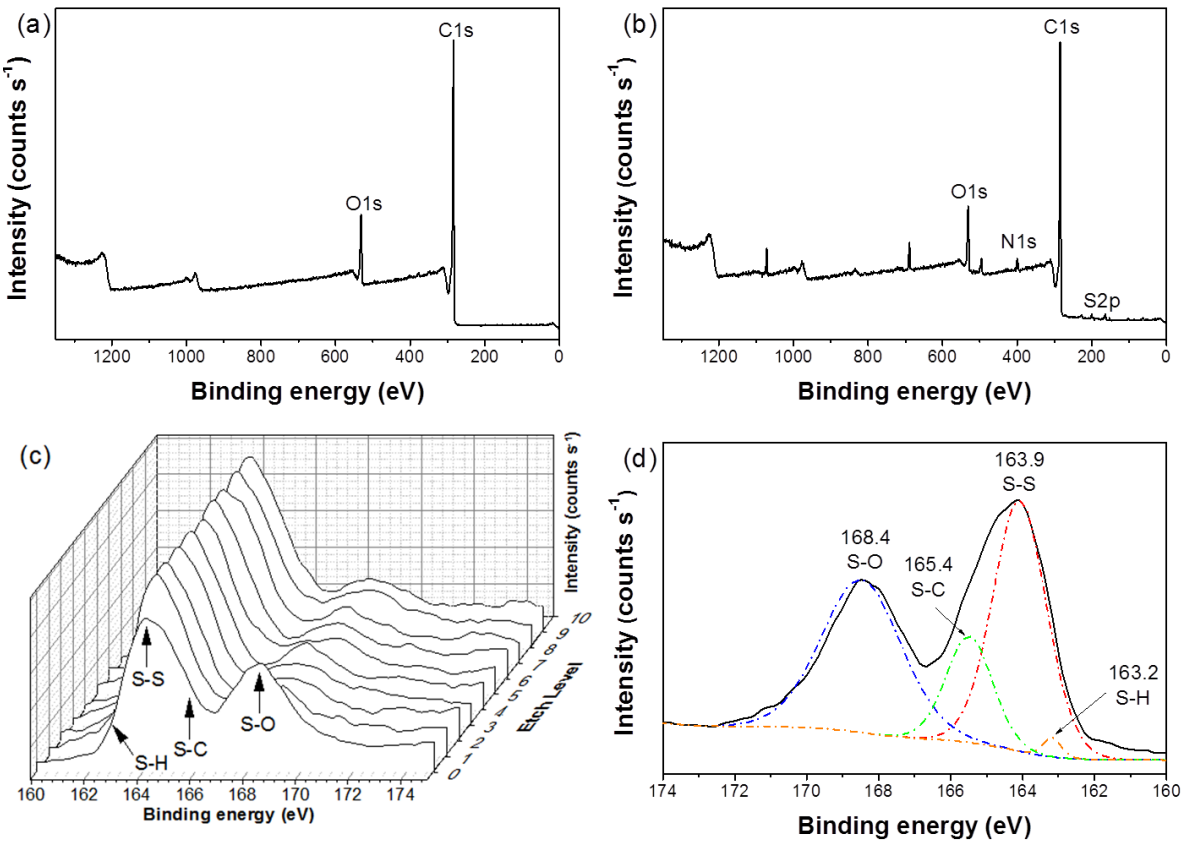

Figure 4.4 X-ray photoelectron spectroscopy data. (a) Bare GAC survey scan. (b) Polymer-grafted DiS-AC survey scan. (c) Depth profile ion-etched S2p scan for DiS-AC (note that the x-axis has been reversed to display peak variation better). (d) Peak deconvolution of S2p scan etch-0 (before etching took place) for DiS-AC (Paper III).

The robustness and thermal stability of the DiS-AC composite was determined by TGA (Figure 4.5). Overall, the weigh drop in raw GAC was roughly 13%, which is similar to a previous study examining melamine grafting with the same types of GAC used in this study (Mines et al. 2017). However, DiS-AC showed an overall drop in weight by roughly 28%, exemplified by an observable correlation in the shape of the drop curve for the pure disulphide polymer, thereby clearly confirming the existence of disulfide polymer in the composite.

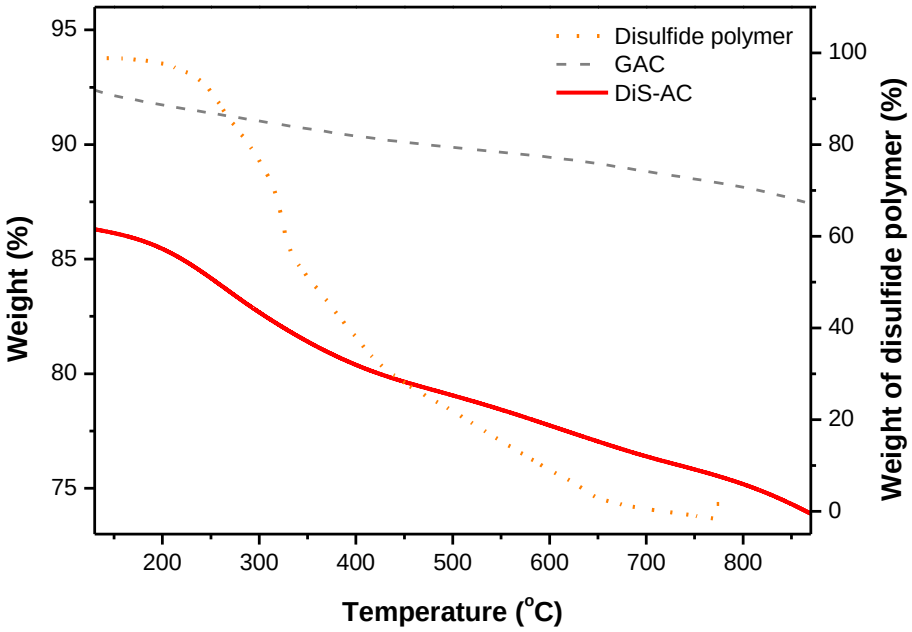

Figure 4.5 Thermo-gravimetric analysis of bare GAC (dashed line), the pure disulphide polymer (dotted line) and the grafted polymer DiS-AC (solid line) (Paper III).

For further confirmation of a grafted polymer, an FT-IR measurement was coupled with the TGA off-gas stream. In Figure 4.6, the spectra of TGA off-gas are plotted with respect to temperature.

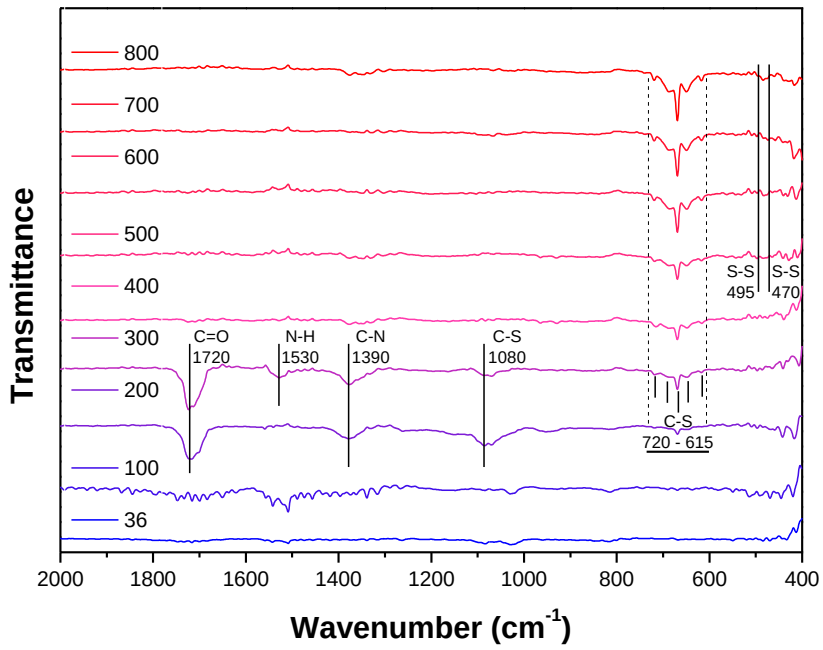

Figure 4.6 TGA-FTIR analysis of DiS-AC, plotted as a function of the TGA analysis temperature (i.e. 36–800 °C) (Paper III).

The discernible peaks are shown from 200°C, since the grafted polymer begins to vaporise at this temperature. At the higher wavenumber range, polymer peaks at

1720 cm^{-1} (C=O), 1530 cm^{-1} (N-H) and 1390 cm^{-1} (C-N) are indicated. At a temperature of around 200–300 °C, a typical series of peaks – attributed to the C-S bond – appears at 1080 cm^{-1} and the range 615–720 cm^{-1}, as observed in other studies (Rao et al. 1964; Halas et al. 2010). Moreover, two weak peaks relating to the S-S disulphide bond are observed at 495 and 470 cm^{-1} and at high temperatures, although the signals for disulphide typically have a very weak signal in IR analysis (Philias & Marsan 1999).

4.1.3 Sorption behaviour study

The sorption isotherm and capacity studies were conducted with eight different concentrations of cadmium. All samples were collected at initial and equilibrium times of 24 hours. The kinetics test followed the isotherm test by scrutinising the sorption of three different concentrations of cadmium solution, with five samples for each concentration. Lastly, pH effects on sorption behaviour were determined by changing the sorption pH from 6 to 8. The results of the isotherm studies were fitted by Langmuir and Freundlich isotherm models (Figure 4.7). The parameters from two models, along with correlation coefficients, are given in Table 4.2.

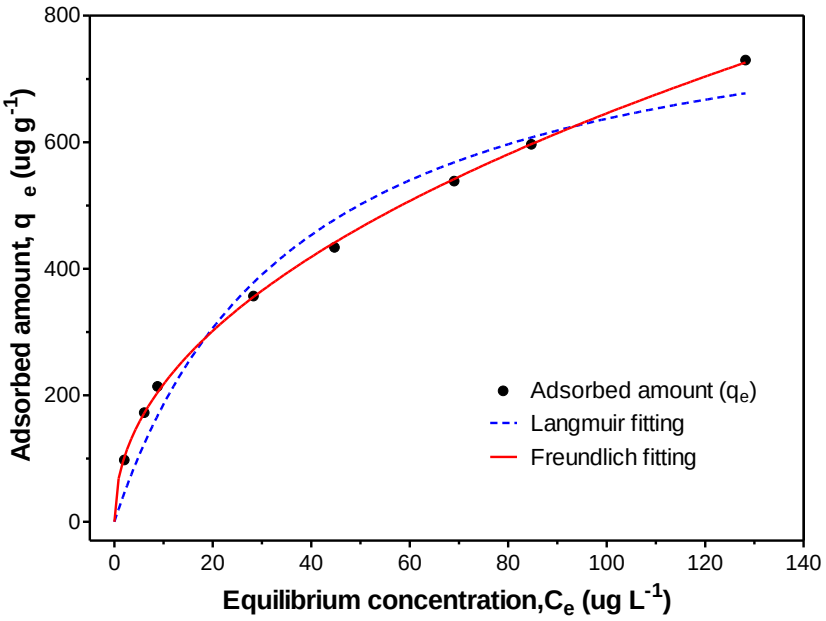

Figure 4.7 Adsorption isotherms of cadmium adsorption on disulphide-linked polymer-grafted carbon substrates (DiS-AC). The red solid line represents the non-linear fitting of data by the Freundlich model, while the blue dashed line represents fitting by the Langmuir model (Paper III).

The DiS-AC sorption experimental plot conformed better with Freundlich fitting according to the correlation coefficient, r^2 = 0.99, while the Langmuir fitting was r^2 = 0.77. Considering differences in the assumptions of the two isotherm models (Hadi et al. 2015), the accordance between the DiS-AC sorption plot and

Freundlich are explained by the inherent randomness of polymers grafted onto the surface of carbon. The low correlation coefficient from the Langmuir isotherm can be explained by the fact that the present work aimed to remove trace amounts of cadmium, which are relevant to stormwater runoff conditions, and so the experimental results cover only the region before the plateau starts from the Langmuir isotherm.

Table 4.2 Parameters corresponding to the Freundlich and the Langmuir sorption isotherm and solid-water partitioning coefficients (K_d) for DiS-AC with comparison of previous literatures (Paper III).

	Freundlich			Langmuir			K_d (L/g)
	K_F	n	R^2	q_m (ug/g)	a_L	R^2	
DiS-AC	73	2.12	0.99	873	0.03	0.96	89.46
GAC	3.28	3.03	0.85	11,980	0.39	0.98	11.78

The Freundlich constant, which is associated with the capacity of the sorbent (Hameed et al. 2007), was 73 [(mg g^{-1})(mg^{-1}) $^{1/n}$] in DiS-AC, which is enormously higher than commonly used sorbents (i.e. GAC and sand) for stormwater filtration (Sansalone 1999; Chen & Wang 2000). The heterogeneity and sorption favourability factor, n, was calculated in this instance from the non-linear fitting of the Freundlich model, and the DiS-AC value shows n = 2.12, which indicates that the sorbent contained a high affinity of adsorbing cadmium ions (Boparai et al. 2011; Jodeh et al. 2014). Moreover, the sorption affinity (K_d) of DiS-AC reached 89 L/g, while the GAC only registered 12 L/g.

Three concentrations of cadmium solutions were selected (0.2 mg/L, 0.35 mg/L and 0.5 mg/L) to observe the sorption kinetics of DiS-AC in different conditions. However, when the replicates of three sorption tests were normalised, the trends were similar (Figure 4.8a). It is suspected that all test metal concentrations were in trace amounts, so there was no diffusion force exerted on sorption. The lowest concentration of cadmium, 0.2 mg/L, was selected for determining and calculating representative kinetics fittings and values. In Figures 4.8b and c, pseudo first-order kinetics and pseudo second-order kinetics are fitted. As a result, both kinetics models are well-fitted on the experimental data, though DiS-AC correlates closer to pseudo second-order kinetics based on the correlation coefficient, which indicates that overall sorption is derived mainly by chemisorption (Ho & McKay 1999). The half-life of cadmium in the solution was observed at 53 min of contact time, in 2g of DiS-AC in 1L of solution. When 4g of activated carbon was applied in the same amount of water, a half-life of 2.5 hours was measured previously (Mohan & Singh 2002). Assuming that kinetics increase proportionally in relation to the amount of adsorbent, DiS-AC in a real-

life stormwater filter (Contech Engineered Solutions 2017; Contech Engineered Solutions 2016) will be expected to remove 97% of cadmium within 10 seconds.

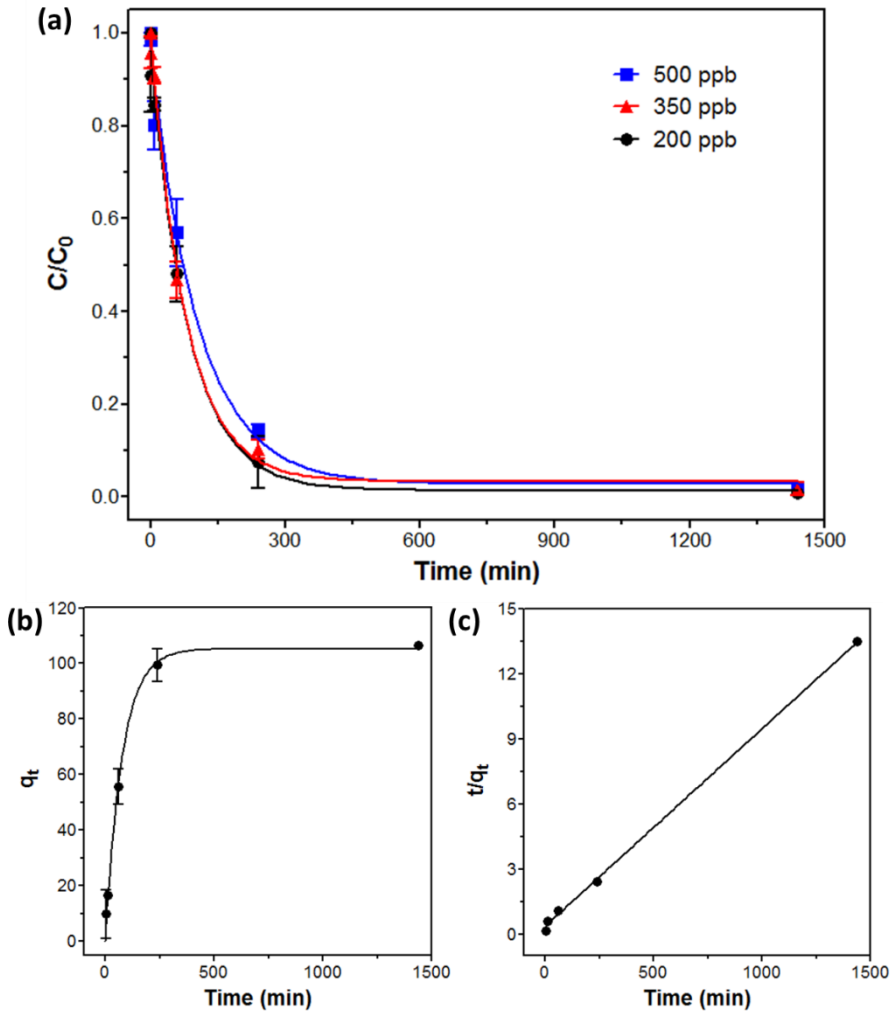

Figure 4.8 (a) Sorption kinetics trends of DiS-AC in batch experiments with 2 g/L dosage at three initial concentrations with normalised y-axes. (b) Pseudo first-order kinetics fitting for 0.2 µg/L cadmium as an initial concentration. (c) Pseudo second-order kinetics fitting of 0.2 µg/L cadmium as an initial concentration. (Error bars represent the standard deviation for replicates) (Paper III).

Sorption tests at different pH conditions were applied for DiS-AC. After 24 hours contact time, which corresponded to equilibrium, the removal percentages of cadmium ions were 87%, 95% and 98% at pH values of 6, 7 and 8, respectively. Among the results, pH 8 showed better sorption behaviour, albeit DiS-AC retained high sorption ability across the overall pH range of 6–8 (Figure 4.9). It is important to note that the pH of urban stormwater runoff fluctuates within the range of pH 6–8 (Jeng et al. 2005), so when DiS-AC is applied for a stormwater filter, it could operate without any need for pre-treatment, in order to adjust for pH levels.

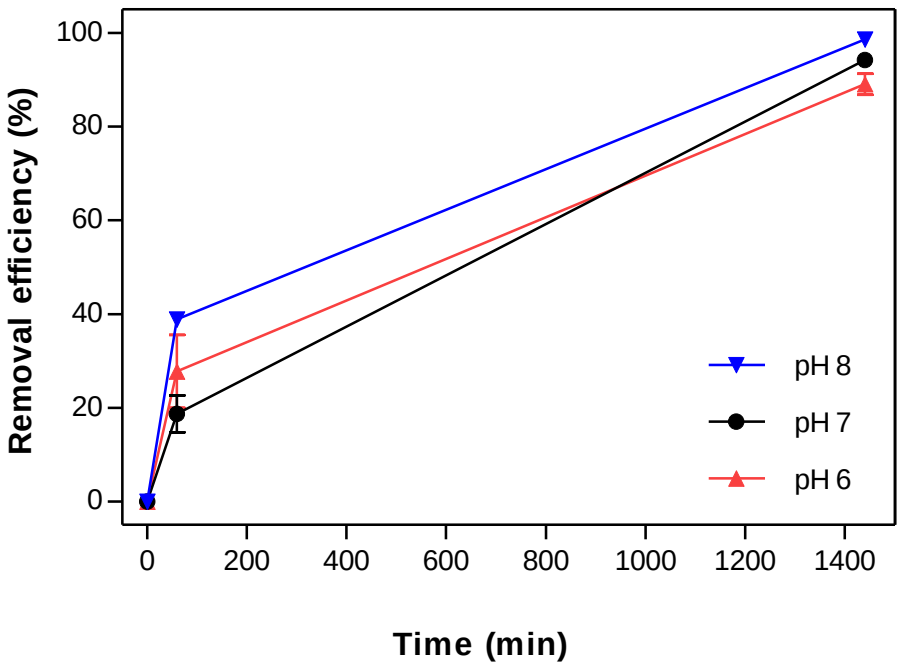

Figure 4.9 Cadmium removal efficiency of DiS-AC at different pH conditions in batch experiment with 2 g/L dosage. Error bars represent the standard deviation for replicates (Paper III).

Additionally, the dependency of the pH of DiS-AC is similar to the behaviour of a disulphide-linked polymer that has been grafted onto DiS-AC (Ko et al. 2017).

4.2 Polymer embedded size-tuneable alginate bead (DiS-algi)

To remove cadmium from stormwater runoff, a new reactive filtration column is introduced in this section. Disulphide-linked polymer particles were stably embedded onto the surface of alginate bead (DiS-algi). In addition, these DiS-algis were placed into a column to simulate a real stormwater treatment filtration column. Overall, DiS-algi has sufficient properties to be suggested as a new cadmium sorption filter material for stormwater runoff.

4.2.1 Preparation of DiS-algi

Disulphide-linked polymers were prepared by adding a strong oxidant into a solution of thiocyanuric acid and stirred overnight. The thiols formed a disulphide linkage through oxidisation, and finally yellowish powdery polymers were obtained. Afterwards, by dropping a solution containing sodium alginate and 1.6 wt% disulphide polymers into a 0.1 M $CaCl_2$ solution, polymer-embedded alginate beads (DiS-algis) were prepared. The final products were washed thoroughly with distilled water several times.

4.2.2 Properties of polymer-embedded alginate beads

Elemental analysis and infrared spectra were measured as well imaging by an optical microscope. The morphology of disulphide polymer, DiS-algi and cross-section images of both bare and DiS-algi beads from optical microscope are illustrated in Figure 4.10. The initial grain size of the disulphide polymer is smaller than 50 µm. After embedding the polymer onto the alginate bead, however, the material increased to around 3 mm, which is similar to the commercialised filter materials in Figures 4.10c and f.

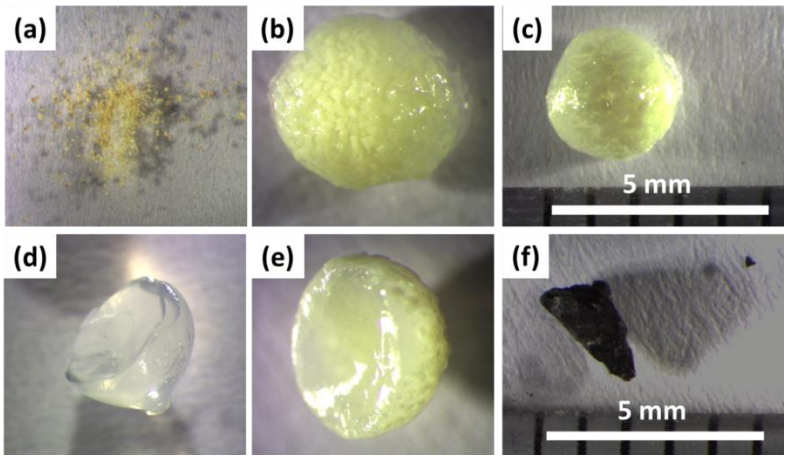

Figure 4.10 Images obtained from optical microscope. (a) Disulphide polymers (b) DiS-algi (c) DiS-algi with size indication (d) cross-section image of a bare alginate bead (d) cross-section of DiS-algi and (f) commercialised granular-activated carbon with size indication (Paper II).

Furthermore, polymers were clearly embedded only on the surface of alginate bead, as shown in Figure 4.10e, thereby indicating that accessibility of heavy metal ions to the active sites of the embedded polymer would not inhibited by the composite size. This is proven by sorption comparison tests between polymers and DiS-algi (Figure 4.11).

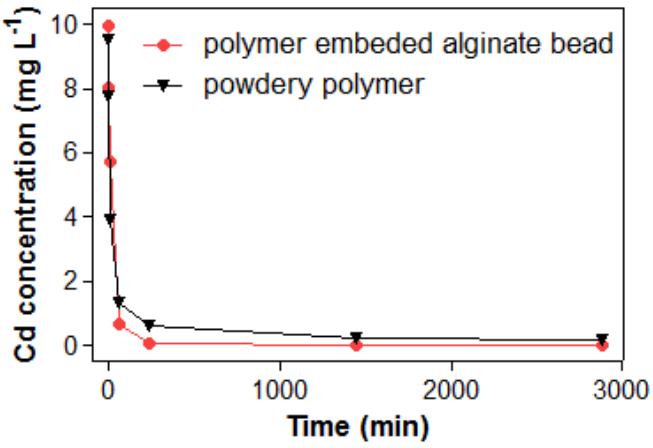

Figure 4.11 Sorption kinetics tests of disulphide polymers and DiS-algi at an initial concentration of 10 mg/L with a 2 g/L sorbent dosage (Paper II).

Comparing IR peaks and elemental analyses, the functionality of disulphide polymers was confirmed. The elemental analysis of disulphide polymer resulted in 19.8% C, 0.4% H, 21.3% N, 52.5% S and 4.0% O, in accordance with the theoretical elemental percentage of disulphide-linked polymer networks (Theoretical C: 19.7%, H: 0.5%, N: 23.0%, S: 52.7% and 4.0% O). The IR spectra in Figure 4.12 show aromatic trithiol stretching peaks at 1466, 1226 and 823 cm^{-1}, while the representative peaks of C=S stretching are apparent at 1120 cm^{-1}. Peaks presenting at 456 and 533 cm^{-1} prove the existence of disulphide linkages in the polymer networks (Ko et al. 2017).

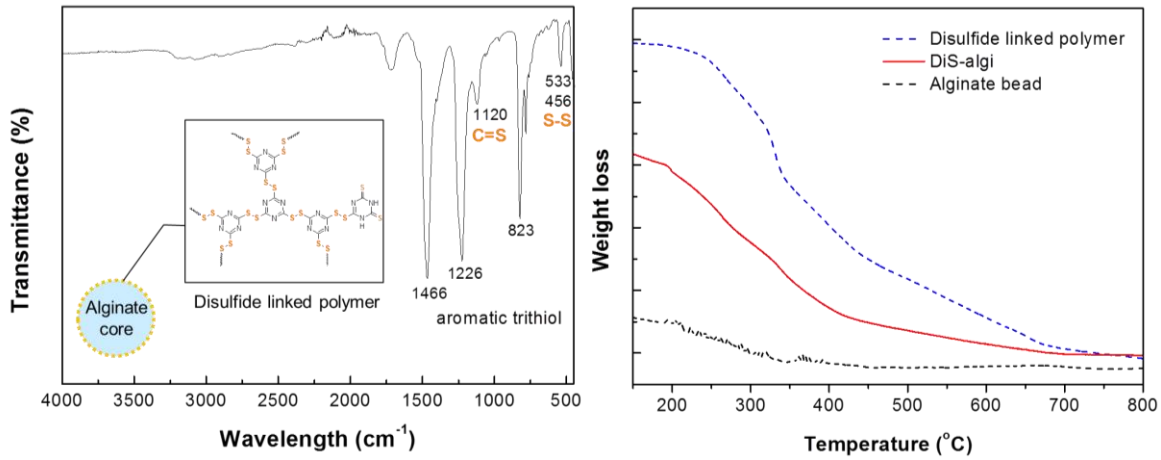

Figure 4.12 Infrared spectra of disulphide-linked polymer networks with an inset schematic of DiS-algi (left). Thermal stability comparison of disulphide-linked polymer, alginate beads and DiS-algi (right). Weight loss before 100 degrees C is ascribed to water evaporation. DiS-algi and alginate bead weight losses are magnified five-fold (Paper II).

Thermogravimetric analysis establishes that DiS-algi follows the stability trends of a disulphide polymer (Figure 4.12). Based on overall physiochemical

characteristics, embedding a functionalised polymer onto the surface of a substrate, without any molecular degradation, is confirmed.

4.2.3 Sorption behaviour study

To determine the sorption behaviour of DiS-algi, isotherm and kinetics tests were conducted in solutions prepared from metal stock with 0.003 M of $NaHCO_3$ buffer solution. The pH range was controlled with 1 M of HCl and NaOH. As a comparison, commercialised GAC was also tested along with DiS-algi. Every test was held in a conical polyethylene (PE) tube, and for the kinetics experiments, six sampling times between 0 and 2,880 mins were selected. Batches were shaken on an end-over-end rotator at 15 rpm, and all filtrates were acidified with 1% HNO_3.

For the sorption isotherm study, experimental data for both DiS-algi and GAC were fitted with the Langmuir isotherm, as shown in Figure 4.13. The maximum sorption capacity was calculated and 22.4 mg/g resulted for DiS-algi. Compared with the GAC, at 11.5 mg/g, two times higher sorption was obtained. Moreover, the Langmuir affinity constant (a_L) of DiS-algi was 31 L/mg, which is nearly 10^3 times higher than the affinity constant of the GAC at 0.03 L/mg.

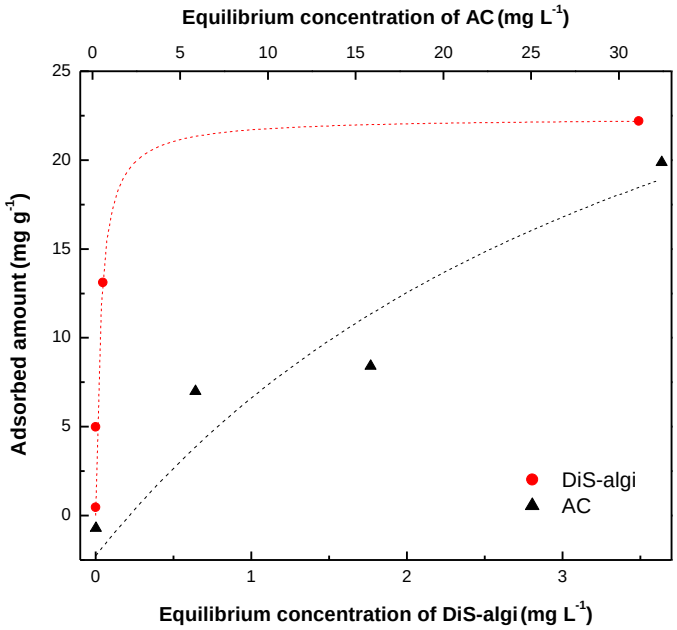

Figure 4.13 Langmuir sorption isotherm of a DiS-algi plot with a fitted line (red), and activated carbon plots with a fitted line (black) from four different initial concentration batch tests (Paper II).

The kinetics studies were conducted at four different cadmium concentrations (Figure 4.14). The sorption kinetics of DiS-algi was faster compared to the GAC, since DiS-algi sorption is derived through not only diffusivity, but also chemical attractions, as confirmed by the kinetics model. The kinetics model fitting shows

that DiS-algi is in good accordance with pseudo second-order kinetics (Figure 4.15).

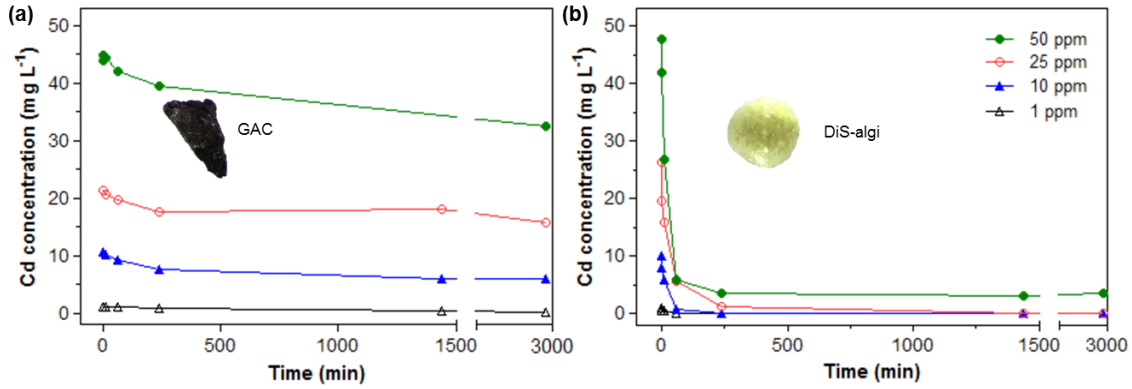

Figure 4.14 Cadmium adsorption kinetics studies of (a) GAC and (b) DiS-algi. Four different initial concentrations of cadmium were compared and differentiated by colour: green, red, blue and black represent 50, 25, 10 and 1 ppm, respectively (Paper II).

Moreover, half of the cadmium ions were removed within 6 min when DiS-algi was introduced into the polluted water. Compared with the half-life of the GAC at 430 mins, DiS-algi has 70 times faster sorption in the same conditions.

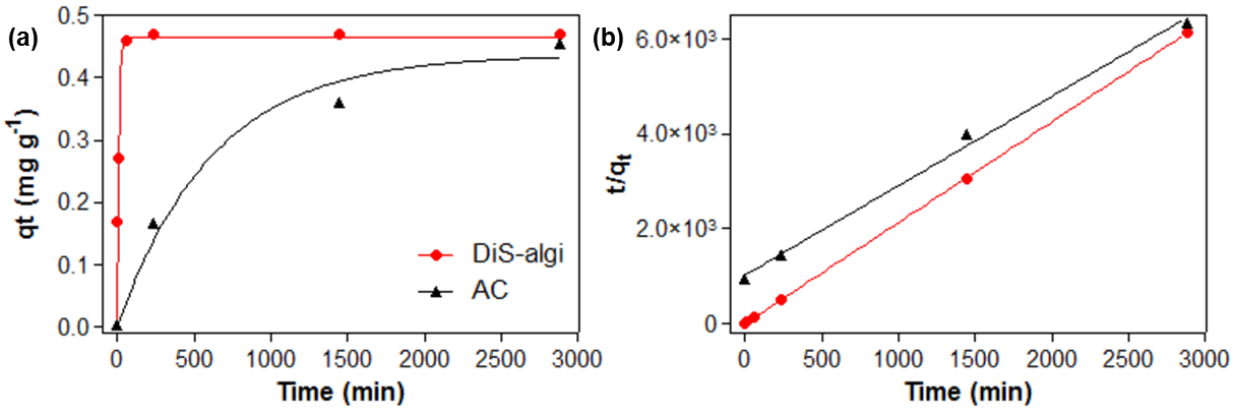

Figure 4.15 Kinetics fitting on DiS-algi and AC plots measured at 1 mg/L initial cadmium concentration. (a) Pseudo first-order kinetics fitting and (b) Pseudo second-order kinetics fitted line (Paper II).

4.2.4 Simulated reactive column

In order to simulate a real stormwater filter, the reactive column was built with DiS-algis. First, to find the optimal flow rate for the test, different flow rates were applied. Cadmium solution was prepared from a 1000 mg/L cadmium stock solution with a 0.003M of $NaHCO_3$ buffer solution. Inflow was controlled at a pH range of 6 to 7 before being fed into the column. As an inert filling layer, sea sands were used, and DiS-algi or GAC were placed between the layers. The peristaltic pump was used to control the flow rates (0.5, and 1 ml/min) and the eluent was filtered using a 0.7 µm glass microfibre filter (Figure 4.16).

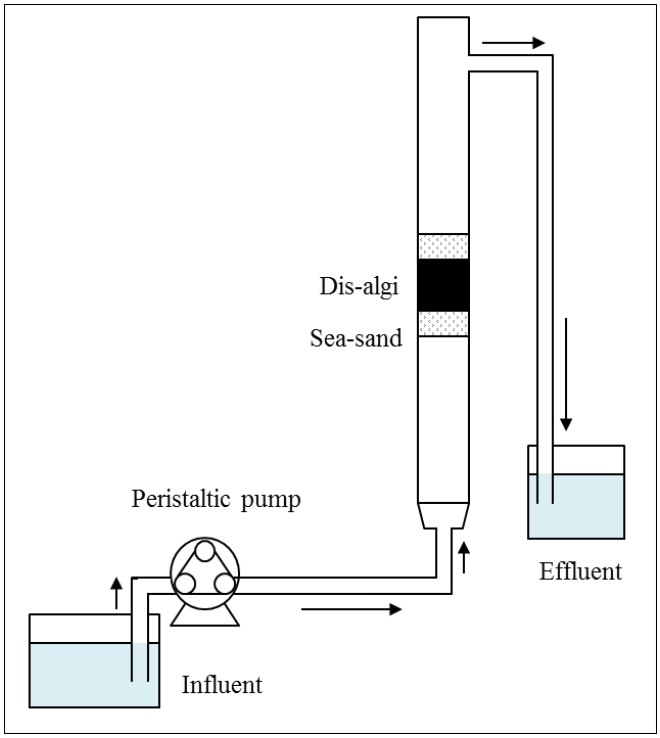

Figure 4.16 Schematic diagram of a lab-scale reactive DiS-algi column. Arrows indicate the direction of flow during the test (Paper II).

The breakthrough time and curve are important properties of fixed bed columns when determining sorption behaviour and parameters for the operation of the column (Ahmad & Hameed 2010)(Malkoc & Nuhoglu 2006). The effective volume (V_{eff}) can be calculated by the following equation:

$$V_{eff} = Qt_{total} \quad (5)$$

where Q is the volumetric flow rate (ml/min) and t_{total} is the total flow time (min).

The area below the breakthrough curve represents the total adsorbed amount of adsorbate in the column (q_{total}) that can be calculated by integrating adsorbed concentrations by function of time, expressed as:

$$q_{total} = \frac{Q}{1000}\int_{t=0}^{t=t_{total}} C_{ad}\, dt \quad (6)$$

where C_{ad} and t are adsorbed concentration (mg/L) and time (min), respectively.

The maximum capacity of the column (q_{eq}) can be determined by the following equation:

$$q_{eq} = \frac{q_{total}}{w} \quad (7)$$

where w is the amount of adsorbent (g).

First, the reactive column and the GAC column were tested with two different flow rates (Figure 4.17). At a high flow rate (1 ml/min), breakthrough points for both columns were not obtained, due to a lack of time for removing cadmium ions from the continuous flow. When the reduced flow rate was applied (0.5 ml/min), the reactive column shows breakthrough point at 137 minutes, while the GAC column took 4 minutes. Thus, a flow rate 0.5 ml/min was used throughout further tests.

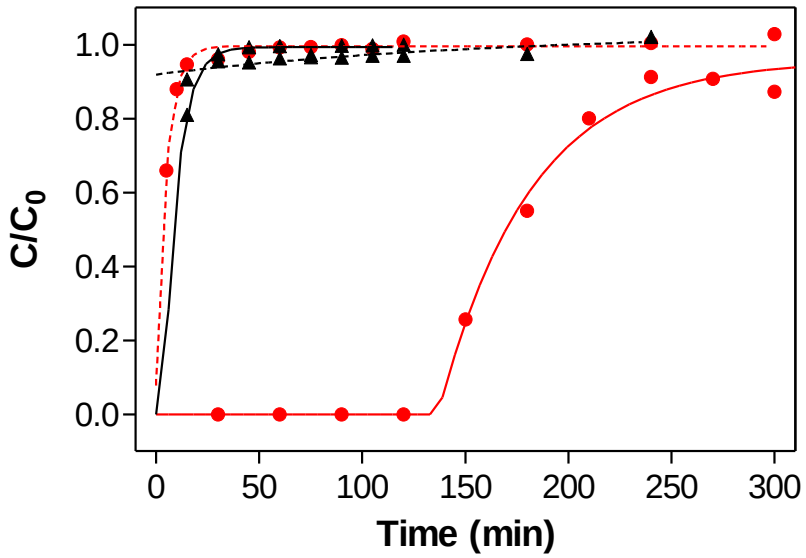

Figure 4.17 Cadmium removal plot in fixed bed column with continuous flow rate 0.5 and 1 mL/min. Both DiS-algi and GAC plots are fitted by non-linear fitting. Red dots represent DiS-algi, black dots for GAC and solid line showing 0.5 mL/min flow rate while dashed line for 1 mL/min flow rate (Paper II).

Other parameters are calculated based on Equations 5-6, meaning that the reactive column had an effective volume of 68.5 mL and 70 µg of total adsorbed cadmium. Moreover, the maximum capacity of the column was 877 µg/g, which is 13 times higher than the GAC column with 64 µg/g capacity.

4.2.5 Regeneration of the reactive column

To be commercialised as a stormwater filter, column reusability is important in terms of cost. To determine its reusability, the reactive column in this instance was flushed with selected solutions, i.e. 0.01 M and 0.1 M of EDTA and 0.1 M of HCl. The flushing flow rate was fixed at 0.5 ml/min. Among the flushing agents, 0.1 M of HCl had a better washing property compared to others. On the other hand, 0.01 M EDTA did not have any washing ability, while 0.1 M EDTA extracted cadmium ions from the column but had high fluctuations in relation to desorption. Therefore, repeated adsorption and desorption tests continued with 0.1

M HCl, while the mass of cadmium in the column was also calculated (Figure 4.18).

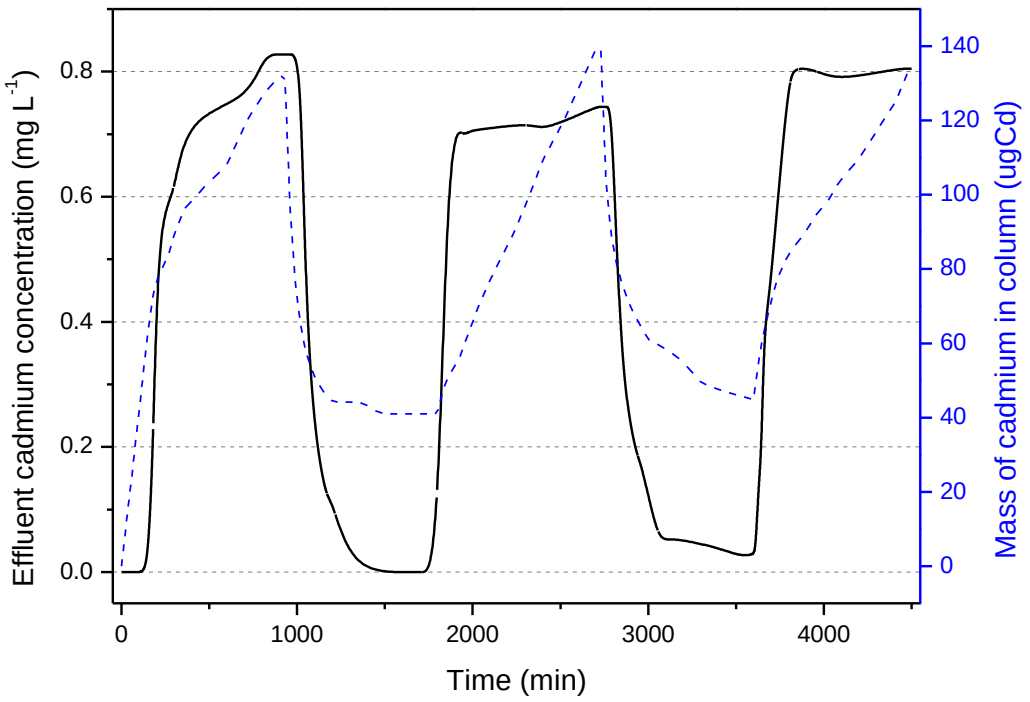

Figure 4.18 Sorption-desorption repeated test on a reactive column, using 0.1 M of HCl as a flushing agent for desorption. Black solid and blue dashed lines indicate effluent cadmium concentrations and the mass of cadmium in the reactive column, respectively (Paper II).

As shown in Figure 4.18, the mass of cadmium in the reactive column decreases slightly, due to the cadmium remaining after the regeneration step. The reactive column uptakes 133 µgCd in the first sorption test and decreases to 98 and 91 µgCd in the second and third sorption tests, respectively. However, after the first run, the cadmium uptake capacity of the column stabilises and breakthrough curves are retained three times in the cyclic sorption tests.

Conclusions

For the efficient sorption of stormwater runoff, functional groups in polymer sorbents represent an imperative parameter. Comparison tests show that the sulphur functionality results in faster heavy metal sorption kinetics and higher sorption capacity, due to hard-acid and hard-base interactions. Moreover, sorbent containing hydrophilicity, derived by polar functional groups could enhance the speed of sorption kinetics regardless of the surface area of the sorbent. Based on these results, three new functionalised polymers have been devised and synthesised. First is disulfide linked polymer designed to contain hydrophilic functional groups and a high percentage of sulphur groups at 52.5% (COP-63). Second is an asymmetric sulphur polymer synthesised by random polymerisation and with 60% sulphur (COP-208). The last polymer, NTA-COP, has been designed specifically for nickel removal. The NTA-COP study only involved a model dimer synthesis test, so it will need to be developed further in the future.

Among the devised polymers, COP-63 was selected and scrutinised in relation to its heavy metal sorption behaviour compared to AC. As a result, COP-63 had maximum sorption capacity similar to high-quality AC on a mass basis, while COP-63 had higher sorption capacity than AC on a surface area basis. From the kinetics tests in a stirred batch, COP-63 showed rapid sorption kinetics with a half-life of 4 min. These tests also confirm that the sorption of COP-63 derived mainly from a chemisorption mechanism. Moreover, pH effect studies proved the chemical interaction between heavy metal and disulphide/thiol sites. The zeta potential of COP-63 and the composition of metal speciation in different pH conditions do indeed affect significantly the sorption of heavy metals. It was observed that the targeted heavy metals, such as copper, cadmium and zinc, have selective binding affinity to COP-63 in the presence of 10 times higher concentrations of alkaline earth metal ions.

Afterwards, two types of sorbent composites were introduced to establish an optimal filter material size. The formulation of first composite, DiS-AC, was proved by various characterisation techniques. From a heavy metal sorption test, DiS-AC had enormously higher sorption affinity than GAC or sand. Additionally, material sorption capacity was screened in different pH conditions and, as a result, DiS-AC sorption capacity covers all of the pH range between 6 and 8, which is in good accordance with stormwater runoff pH conditions. Another composite, DiS-algi, also showed high maximum sorption capacity and sorption affinity compared to a conventional sorption material, in this case GAC. Moreover, the DiS-algi sorption mechanism proved good in relation to chemisorption, via a pseudo-second order kinetics model that gives rapid sorption kinetics with 6 mins of cadmium half-life time. With DiS-algi, a reactive column test for simulating

stormwater runoff filter was conducted. From the breakthrough tests, 877 μg/g maximum capacity for the reactive column and 2 hours' breakthrough time were observed. Moreover, column regeneration was also tested, to prove its reusability.

Overall, during the PhD project, brand new polymer composites were created and confirmed as effective filter materials for stormwater runoff treatment applications.

Further studies will need to be done for the proposed composites, before being applied to real-life stormwater filters. First, even though the stability of the attached polymer has been confirmed by TGA, practical stability should be checked by analysing the effluent of the filter. Second, a scale-up of the reactive column would be needed, to find the optimal bed depth of the filter and the flow rate of the inlet.

References

Van der Aa, L.T.J. et al., 2002. Nitrification in rapid sand filter: Phosphate limitation at low temperatures. *Water Science and Technology: Water Supply*, 2(1), pp.37–46.

Abou-Gamra, Z.M. & Ahmed, M.A., 2015. TiO2 nanoparticles for removal of malachite green dye from waste water. *Advances in Chemical Engineering and Science*, 5(5), pp.373–388.

Ahmad, A.A. & Hameed, B.H., 2010. Fixed-bed adsorption of reactive azo dye onto granular activated carbon prepared from waste. *Journal of Hazardous Materials*, 175(1–3), pp.298–303.

Ali, I. & Gupta, V.K., 2006. Advances in water treatment by adsorption technology. *Nature protocols*, 1(6), pp.2661–2667.

Allen, S.J., Mckay, G. & Porter, J.F., 2004. Adsorption isotherm models for basic dye adsorption by peat in single and binary component systems. *Journal of Colloid and Interface Science*, 280(2), pp.322–333.

Azzi, V. et al., 2017. Lactuca sativa growth in compacted and non-compacted semi-arid alkaline soil under phosphate fertilizer treatment and cadmium contamination. *Soil and Tillage Research*, 165, pp.1–10.

Bhatnagar, A. et al., 2013. An overview of the modification methods of activated carbon for its water treatment applications. *Chemical Engineering Journal*, 219, pp.499–511.

Boparai, H.K., Joseph, M. & Carroll, D.M.O., 2011. Kinetics and thermodynamics of cadmium ion removal by adsorption onto nano zerovalent iron particles. *Journal of Hazardous Materials*, 186(1), pp.458–465.

Byun, J. et al., 2017. Reversible water capture by a charged metal-free porous polymer. *Polymer (United Kingdom)*, 126, pp.308–313.

Castner, D.G., Hinds, K. & Grainger, D.W., 1996. X-ray photoelectron spectroscopy sulfur 2p study of organic thiol and disulfide binding interactions with gold surfaces. *Langmuir*, 12(21), pp.5083–5086.

Cederkvist, K. et al., 2016. Controlling stormwater quality with filter soil—event and dry weather testing. *Water*, 8(8), p.349.

Chen, J.P. et al., 2005. Gravity Filtration. *Physicochemical Treatment Processes*, 3(13), pp.501–543.

Chen, J.P. & Wang, X., 2000. Removing copper , zinc , and lead ion by granular activated carbon in pretreated fixed-bed columns. *Separation and Purification Technology*, 19, pp.157–167.

Contech Engineered Solutions, L., 2016. *Media cartridge filtration system drawing specifications*, Portland, OR 97220.

Contech Engineered Solutions, L., 2017. *Safety data sheet*, Portland, OR 97220.

Crini, G., 2005. Recent developments in polysaccharide-based materials used as adsorbents in wastewater treatment. *Progress in Polymer Science (Oxford)*, 30(1), pp.38–70.

Dai, M., 1994. The effect of zeta potential of activated carbon on the adsorption of dyes from aqueous solution: I. the adsorption of cationic dyes: methyl green and methyl violet. *Journal of Colloid and Interface Science*, 164, pp.223–228.

Descostes, M. et al., 2000. Use of XPS in the determination of chemical environment and oxidation state of iron and sulfur samples: Constitution of a data basis in binding energies for Fe and S reference compounds and applications to the evidence of surface species of an oxidized py. *Applied Surface Science*, 165(4), pp.288–302.

Fang, Q.-R. et al., 2010. Recent advances in the study of mesoporous metal-organic frameworks. *Comments on Inorganic Chemistry*, 31(5–6), pp.165–195.

Field, R., Brown P., M. & Vilkelis V., W., 1994. *Stormwater pollution abatement technologies*, US Environmental Protection Agency, Cincinnati, OHIO 45268.

Fletcher, T. et al., 2004. Stormwater flow and quality, and the effectiveness of non-proprietary stormwater treatment measures : a review and gap analysis. *Technical report*, (December), pp.1–171.

Foo, K.Y. & Hameed, B.H., 2010. Insights into the modeling of adsorption isotherm systems. *Chemical Engineering Journal*, 156, pp.2–10.

Genç-Fuhrman, H., Mikkelsen, P.S. & Ledin, A., 2016. Simultaneous removal of As, Cd, Cr, Cu, Ni and Zn from stormwater using high-efficiency industrial sorbents: Effect of pH, contact time and humic acid. *Science of the Total Environment*, 566–567, pp.76–85.

Gittleman, M. et al., 2017. Estimating stormwater runoff for community gardens in New York City. *Urban Ecosystems*, 20(1), pp.129–139.

Göbel, P., Dierkes, C. & Coldewey, W.G., 2007. Storm water runoff concentration matrix for urban areas. *Journal of Contaminant Hydrology*, 91(1–2), pp.26–42.

Hadi, P. et al., 2015. Aqueous mercury adsorption by activated carbons. *Water Research*, 73, pp.37–55.

Halas, N.J. et al., 2010. Compositions for surface enhanced infrared absorption spectra and methods of using same.

Hameed, B.H., Din, A.M. & Ahmad, A.L., 2007. Adsorption of methylene blue onto bamboo-based activated carbon: kinetics and equilibrium studies. *Journal of hazardous materials*, 141(3), pp.819–825.

Ho, T.L., 1975. The Hard Soft Acids Bases (HSAB) Principle and Organic Chemistry. *Chemical Reviews*, 75(1), pp.1–20.

Ho, Y.S. & McKay, G., 1999. Pseudo-second order model for sorption processes. *Process Biochemistry*, 34(5), pp.451–465.

Jeng, H.A.C. et al., 2005. Impact of urban stormwater runoff on estuarine environmental quality. *Estuarine, Coastal and Shelf Science*, 63, pp.513–526.

Jodeh, S. et al., 2014. Adsorption of some organic phenolic compounds using activated carbon from cypress products. *Journal of Chemical and Pharmaceutical Research*, 6(2), pp.713–723.

Ko, D. et al., 2017. Selective removal of heavy metal ions by disulfide linked polymer networks. *Journal of Hazardous Materials*, 332, pp.140–148.

Lai, J. et al., 2006. Study on hydrophilicity of polymer surfaces improved by plasma treatment. *Applied Surface Science*, 252(10), pp.3375–3379.

Lauer, S.A. & Nolan, J.P., 2002. Development and characterization of Ni-NTA-bearing microspheres. *Cytometry*, 48(3), pp.136–145.

Lemire, J.A., Harrison, J.J. & Turner, R.J., 2013. Antimicrobial activity of metals mechanisms, molecular targets and applications. *Nature Reviews Microbiology*, 11(6), pp.371–384.

Lin, D.-Q. et al., 2003. Biomass/adsorbent electrostatic interactions in expanded bed adsorption: a zeta potential study. *Biotechnology and bioengineering*, 83, pp.149–157.

LoPachin, R.M. et al., 2012. Application of the hard and soft, acids and bases (HSAB) theory to toxicant–target interactions. *Chemical Reserch in Toxicology*, 10025(2), pp.239–251.

Lu, W. et al., 2012. Polyamine-tethered porous polymer networks for carbon dioxide capture from flue gas. *Angewandte Chemie - International Edition*, 51(30), pp.7480–7484.

Malkoc, E. & Nuhoglu, Y., 2006. Fixed bed studies for the sorption of chromium(VI) onto tea factory waste. *Chemical Engineering Science*, 61(13), pp.4363–4372.

McDonald, T.M. et al., 2012. Capture of carbon dioxide from air and flue gas in the alkylamine-appended metal-organic framework mmen-Mg 2(dobpdc). *Journal of the American Chemical Society*, 134(16), pp.7056–7065.

Mines, P.D. et al., 2017. Covalent organic polymer functionalization of activated carbon surfaces through acyl chloride for environmental clean-up. *Chemical Engineering Journal*, 309, pp.766–771.

Mines, P.D. et al., 2016. Nanoporous networks as effective stabilisation matrices for nanoscale zero-valent iron and groundwater pollutant removal. *Journal of Materials Chemistry A*, 4(2), pp.632–639.

Mohan, D. & Singh, K.P., 2002. Single- and multi-component adsorption of cadmium and zinc using activated carbon derived from bagasse - an agricultural waste. *Water Research*, 36, pp.2304–2318.

Morsi, R.E. & Elsabee, M.Z., 2015. Polyaniline nanotubes: mercury and competative heavy metals uptake. *American Journal of Polymer Science*, 5(1), pp.10–17.

Patel, H.A. et al., 2013. Highly stable nanoporous sulfur-bridged covalent organic polymers for carbon dioxide removal. *Advanced Functional Materials*, 23(18), pp.2270–2276.

Patel, H.A. & Yavuz, C.T., 2015. Highly optimized CO2 capture by inexpensive nanoporous covalent organic polymers and their amine composites. *Faraday Discuss.*, 183, pp.401–412.

Patel, H.A., Yavuz, M.S. & Yavuz, C.T., 2014. Exceptional organic solvent uptake by disulfide-linked polymeric networks. *RSC Advances*, 4(46), p.24320.

Philias, J.-M. & Marsan, B., 1999. FTIR spectroscopic study and thermal and electrical properties of polymer electrolytes containing a cesium thiolate/disulfide redox couple. *Electrochimica Acta*, 44(14), pp.2351–2363.

Pitt, R., Maestre, A. & Morquecho, R., 2004. The national stormwater quality database (NSQD, version 1.1). *1st Annual Stormwater*, pp.1–9.

Rao, C.N.R., Venkataraghavan, R. & Kasturi, T.R., 1964. Contribution to the infrared spectra of organosulphur compounds. *Canadian Journal of Chemistry*, 42, pp.36–42.

Roy, A. & Bhattacharya, J., 2013. A binary and ternary adsorption study of wastewater Cd(II), Ni(II) and Co(II) by r-Fe2O3 nanotubes. *Separation and Purification Technology*, 115, pp.172–179.

Sabin, L.D. et al., 2005. Contribution of trace metals from atmospheric deposition to stormwater runoff in a small impervious urban catchment. *Water Research*, 39(16), pp.3929–3937.

Sancey, B. et al., 2011. Heavy metal removal from industrial effluents by sorption on cross-linked starch: Chemical study and impact on water toxicity. *Journal of Environmental Management*, 92(3), pp.765–772.

Sansalone, J.J., 1999. Adsorptive infiltration of metals in urban drainage - Media characteristics. *Science of the Total Environment*, 235(1–3), pp.179–188.

Schwartz, D., Sample, D.J. & Grizzard, T.J., 2017. Evaluating the performance of a retrofitted stormwater wet pond for treatment of urban runoff. *Environmental Monitoring and Assessment*, 189(6).

Shin, B.Y. et al., 2007. Sulfur-functionalized mesoporous carbon. *Advanced Functional Materials*, 17, pp.2897–2901.

Tingaut, P., Hauert, R. & Zimmermann, T., 2011. Highly efficient and straightforward functionalization of cellulose films with thiol-ene click chemistry. *Journal of Materials Chemistry*, 21(40), p.16066.

Wan Ngah, W.S. & Hanafiah, M.A.K.M., 2008. Removal of heavy metal ions from wastewater by chemically modified plant wastes as adsorbents: A review. *Bioresource Technology*, 99(10), pp.3935–3948.

Xu, X. et al., 2005. Influence of moisture on CO2 separation from gas mixture by a nanoporous adsorbent based on polyethylenimine-modified molecular sieve MCM-41. *Industrial and Engineering Chemistry Research*, 44(21), pp.8113–8119.

Yang, Y.Y. & Toor, G.S., 2017. Sources and mechanisms of nitrate and orthophosphate transport in urban stormwater runoff from residential catchments. *Water Research*, 112, pp.176–184.

Zhang, Y. et al., 2008. Zeta potential: A surface electrical characteristic to probe the interaction of nanoparticles with normal and cancer human breast epithelial cells. *Biomedical Microdevices*, 10(2), pp.321–328.

Zhang, Z. et al., 2011. Organic semiconductor for artificial photosynthesis: water splitting into hydrogen by a bioinspired C 3 N 3 S 3 polymer under visible light irradiation. *Chem. Sci.*, 2(9), pp.1826–1830.

Zhou, G. et al., 2016. Rapid and efficient treatment of wastewater with high-concentration heavy metals using a new type of hydrogel-based adsorption process. *Bioresource Technology*, 219, pp.451–457.

Papers

I **Ko D.**, Lee J., Patel H.A., Jakobsen M.H., Hwang Y., Yavuz C.T., Hansen H.C.B., Andersen H.R. (2017). Selective removal of heavy metal ions by disulfide linked polymer networks. *Journal of Hazardous Materials*, 332:140-148

II **Ko D.**, Kim H., Lee H., Yavuz C.T., Andersen H.R., Hwang Y. (2017). Applicability of disulfide-polymer particles surface embedded on alginate beads for cadmium removal from airport derived stormwater. *Submitted – Journal of Hazardous Materials.*

III **Ko D.**, Mines P.D., Jakobsen M.H., Yavuz C.T., Hansen H.C.B., Andersen H.R. (2017). Disulfide polymer grafted composites for heavy metal removal from stormwater runoff. *Chemical Engineering Journal (under review).*

The Department of Environmental Engineering (DTU Environment) conducts science-based research within six sections: Atmospheric Environment, Environmental Chemistry, Residual Resource Engineering, Urban Water Systems, Water Resources Engineering, Water Technology. The department dates back to 1865, when Ludvig August Colding, the founder of the department, gave the first lecture on sanitary engineering as response to the cholera epidemics in Copenhagen in the late 1800's.

Department of Environmental Engineering
Technical University of Denmark

DTU Environment
Bygningstorvet, Building 115
2800 Kgs. Lyngby
Tlf. +45 4525 1600
Fax +45 4593 2850

www.env.dtu.dk